COMPARATIVE STUDY OF RSS-BASED COLLABORATIVE LOCALIZATION METHODS IN WIRELESS SENSOR NETWORKS

Avanthi Koneru, B.Tech.

Thesis Prepared for the Degree of

MASTER OF SCIENCE

UNIVERSITY OF NORTH TEXAS

December 2006

APPROVED:

Xinrong Li, Major Professor
Robert Akl, Committee Member
Shengli Fu, Committee Member
Yan Huang, Committee Member
Murali Varanasi, Committee Member
Krishna Kavi, Chair of the Department of Computer Science and Engineering
Oscar N. Garcia, Dean of the College of Engineering
Sandra L. Terrell, Dean of the Robert B. Toulouse School of Graduate Studies

Koneru, Avanthi, Comparative Study of RSS-Based Collaborative Localization Methods in Wireless Sensor Networks, Master of Science (Computer Science and Engineering), December 2006, 92 pp., 1 table, 41 figures, 48 references.

In this thesis two collaborative localization techniques are studied: multidimensional scaling (MDS) and maximum likelihood estimator (MLE). A synthesis of a new location estimation method through a serial integration of these two techniques, such that an estimate is first obtained using MDS and then MLE is employed to fine-tune the MDS solution, was the subject of this research using various simulation and experimental studies. In the simulations, important issues including the effects of sensor node density, reference node density and different deployment strategies of reference nodes were addressed. In the experimental study, the path loss model of indoor environments is developed by determining the environment-specific parameters from the experimental measurement data. Then, the empirical path loss model is employed in the analysis and simulation study of the performance of collaborative localization techniques.

ACKNOWLEDGEMENTS

This work would not have been possible without the help, guidance and support of my advisor Dr. Xinrong Li. I would like to express my heartfelt thanks to him for inspiring, encouraging and teaching me over the past year. I would like to extend my gratitude to Dr. Murali Varanasi, for constantly inspiring me to do my best. I owe a great deal of thanks to Dr. Robert Akl, Dr. Shengli Fu and Dr. Yan Huang for their time, patience and insightful comments on my work.

I would like to thank all my colleagues and friends who have made my stay at UNT fun. I'd like to thank Sri for being my personal cheerleader and for believing in me more than I did myself.

I am very grateful to my Amma, Daddy and Akka without whom I would be nothing. They are the force that drives me, fills me and makes me.

CONTENTS

LIST OF TABLES

LIST OF FIGURES

CHAPTER 1

INTRODUCTION

1.1. Introduction to Wireless Sensor Networks

Recent technological advances in micro-electro-mechanical systems (MEMS) integrated circuit (IC) design and radio frequency (RF) has led to the manufacturing of low power electronic devices embedded with on-board processing, storage, wireless communication and sensing capabilities. Such miniature, battery-powered devices, known as wireless sensor nodes, have greatly extended our ability to monitor and control the physical environment [1-3]. The sensors attached to the wireless nodes enable the measurement of physical, chemical, geological, environmental or biological parameters of interest. The wireless sensor nodes can communicate among themselves to form ad hoc networks to collect and share information. Key characteristics of a wireless sensor node are small physical size, low power consumption, limited processing power, short-range communication and a limited storage space among many others. Dense deployments of wireless sensor networks in the physical world will enable us to monitor our environment with a resolution never witnessed before.

Wireless sensor networks can work collaboratively to form root-based collection trees to collect data from the entire network and log it to a base station or root, which is typically a computer. The sensor field can be as varied as a lake, a volcanic mountain, a military battlefield, a state park or a habitat reserve where manual surveillance is difficult

and at times impossible. Figure 1.1 shows an example of wireless sensor networks. The lines in Fig.1.1 represent communication links between nodes, which are typically wireless. Each of the sensor nodes forwards the sensed data to the base station either directly or via their neighboring nodes. The data is logged directly or remotely to a data-collection equipment such as a personal computer.

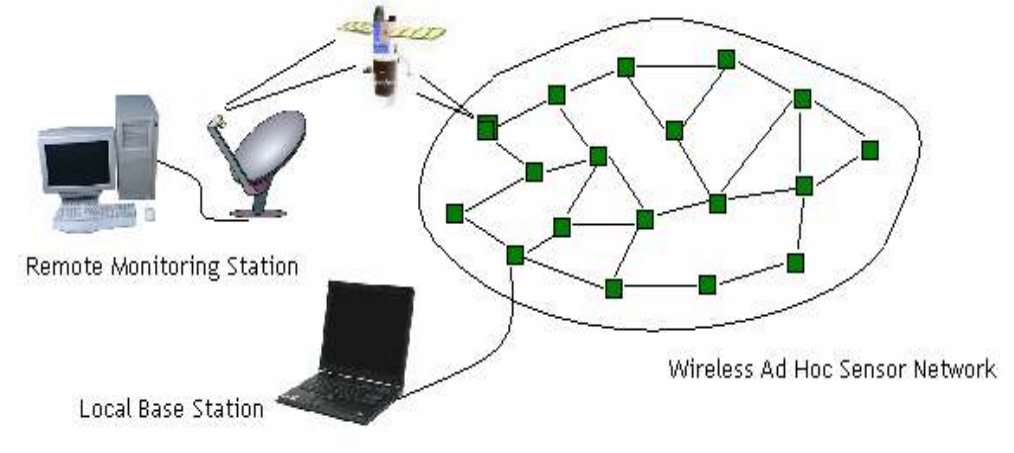

FIGURE 1.1. An example of wireless sensor networks. Sensor nodes sense the environment and send the observation data to a base station for various applications.

Most of the wireless sensor network applications entail knowledge of the location of the individual wireless sensor nodes in order to benefit from the information they sense. An instant detection of the event is of no use if the geographical context of the event is unknown [4]. Hence, the position of the node which generated the event should be known before-hand or computed instantaneously. Traditional location finding systems are not suitable for wireless sensor networks due to several resource constraints in wireless sensor networks. This thesis addresses the challenging issue of localization in wireless sensor networks.

1.2. Localization in Wireless Sensor Networks

To better understand the importance of localization in wireless sensor networks consider that wireless sensor networks are used to regularly monitor forests by deploying numerous event-driven inexpensive sensor nodes that report to the base station once a dramatic change in temperature is noticed, as in the case of a forest fire. Such large-scale deployment of wireless sensor networks necessitates the knowledge of geographical location of the sensor nodes to answer many critical questions such as, "where was the temperature surge reported?" Finding the location of a node accurately, can lead to the realization of several interesting applications like geographic routing [5], where queries pertaining to nodes in a geographical area, are directed to the target nodes in the specific area, saving the energy of the network which would otherwise be wasted in flooding. Reliable localization is also needed to design new energy-efficient location-based techniques for multihop routing, data mining, data fusion, and autonomic calibration in large-scale sensor networks. For example, the use of sensor's location information can significantly reduce the complexity of routing tables and algorithms in large-scale sensor networks [6]. Embedding location finding systems on wireless sensor nodes without increasing the cost of a node can open a whole new window of interesting domains where wireless sensor networks can be utilized. Such systems can be used to track and secure inventory in large warehouses, locate personnel around an office, track people with special needs or elderly in a health care facility, locate tanks or soldiers in the battlefield or for a temporal analysis of animal behavior in natural habitats. Most of these applications can be categorized as target tracking and are not very different from localization. Target tracking applications need location finding systems to exactly pin-

point the location of an emergent event. In tracking applications a sensor grid or bed is setup to observe a phenomenon like the passage of a vehicle or a tank in a battlefield. All of the sensors detecting the event send information back to the base station, where the data is consolidated to identify the path of the enemy tank. The first step of target tracking however, is to localize the sensor bed precisely. The apparent significance of localization in wireless sensor networks has evoked a lot of interest in the research community to find location estimation techniques which can perform accurate localization.

1.3. Motivation of the Thesis

Existing location finding systems like the global positioning satellite (GPS), a satellite-based radio navigation system, cannot be used for wireless sensor networks since embedding a GPS on each of the sensor nodes is highly impractical and raises the cost of a large-scale deployment outrageously. GPS receivers do not work in indoor environments due to an absence of direct visual contact with the satellites. A large-scale deployment also rules out hand-placement or manually recording the positions of the sensor nodes due to the sheer number of the nodes. And hand-placement is very impractical in cases where the positions of the sensors might change due to displacement by external factors like wind, animals or humans. Also, depending on the kind of deployment, it cannot be predicted before hand where the sensor nodes might end up, since the sensors could be dropped from an unmanned air vehicle (UAV) or strewn from a boat. In other cases like inventory management, sensor nodes may not be immobile. Therefore, there is a need for an automatic localization system which computes locations on the fly during the start up of the network or whenever necessary.

More often than not, localization is not the prime reason for a sensor network deployment. They are deployed specifically to closely monitor a phenomenon of interest. Hence, there is great need for a light-weight localization technique which does not demand any additional hardware and is not very resource consuming. This thesis concentrates on a location estimation technique which utilizes the received signal strength (RSS) of a message to estimate the distance between sensor nodes. Using RSS solves two of the problems that are aforementioned: it reduces the cost involved and eliminates the need of additional hardware, keeping the physical size unaltered. Though RSS is touted as a perfect solution for inexpensive deployments, it comes at a cost of imprecision. RSS is not the best available alternative for accurate distance estimates, due to a number of factors such as multipath fading, interference and shadowing among others.

1.4. Objectives of the Thesis

The main goal of this thesis is to design and formulate a collaborative localization algorithm which accurately computes the location estimates of a sensor network, through an optimum usage of resources. Key issues in the localization problem are identified and an investigation of the existing location finding systems is conducted. An extensive literature survey in location finding systems reveals that most of the location finding algorithms are non-collaborative in nature. Collaborative localization techniques exploit the networking capabilities of wireless sensor networks for efficient cooperation among sensor nodes. The first objective of this thesis is to conduct an extensive study of the challenges in designing a localization system in resource-constrained wireless sensor networks.

Sensor networks are severely resource-constrained due to various constraints such as miniature size, low-complexity, limited battery power, and limited communication and computation capacities. Thus, efficient collaboration among sensor nodes is needed to perform complex monitoring and processing tasks using low-complexity sensor nodes. Optimal collaboration among sensor nodes can also significantly improve the efficiency of sensing and processing in sensor networks. Reliable localization in complex environment with resource constrained sensor network is a challenging task [7]. Collaborative signal processing techniques are an efficient way of reliable localization in a resource-constrained sensor network. Due to the inherent advantages of collaborative localization methods, two such techniques are studied in detail: multidimensional scaling (MDS) [9], [10] and maximum likelihood estimator (MLE) [8]. From the theoretical formulation of the RSS-based localization problem, it is seen that MLE appears more appropriate than the MDS method. However, the performance of the techniques is analyzed by subjecting them to a variety of simulation scenarios. The second objective of our thesis is to test the validity of these algorithms rigorously through simulations.

The performance of an algorithm cannot be validated conclusively until the algorithm is tested in an experimental setup, because simulation conditions cannot model anomalies in ranging data as vividly as a practical setup. It also cannot model random signal shadowing or fading effects inherent in signal propagation. The localization techniques studied in this thesis are based on the distance estimates obtained from the received signal strength (RSS) of a message exchanged between two sensor nodes. Reliable location estimation based on RSS depends largely on an accurate modeling of the path loss characteristic of the radio propagation channels. In most of the existing

studies of the RSS–based localization methods, the path loss model is assumed be known apriori either by assuming a perfect free-space environment or by extensive measurements and modeling of the channel before deployment of the localization system. The third objective of this thesis is to study the characteristics of the radio propagation channel and its impact on the performance of the algorithms. An extensive measurement campaign in different environments should uncover the problems in using RSS to compute a distance estimate. As will be shown later on, the radio propagation channel makes it very difficult to obtain an exact translation factor for the conversion of power-loss of the signal to an accurate distance estimate.

1.5. Contributions of the Thesis

In this thesis the issues of the localization problem are established by conducting a study of a wide variety of existing location finding systems. This forms a background to our research and provides insights into how the solution is to be designed. The details of existing localization systems and a framework of our solution can be found in Chapter 2.

Theoretical formulation of the three collaborative localization techniques, MDS, MLE and MDS-MLE can be seen in Chapter 3. Theoretical formulation shows that MLE is more suitable for localization problem than MDS, which converges to a rough estimate of the positions of the nodes. However, a comparative study of MDS and MLE through simulations showed that MLE performs better than MDS only in cases where the initial estimate is close to the final configuration. This comparative study motivated us to integrate the two algorithms to produce a third algorithm called MDS-MLE such that MLE fine-tunes an initial MDS estimate. This comparative study can be found in the Chapter 4. Initially, simulations are conducted to verify the performance of the algorithm

by assuming the values of environment-specific parameters. Different sensor node configurations are used to test the performance of the algorithms in various settings such as high density sensor fields, sparsely spread sensor field, high density reference node density etc. This study provides statistical simulation results of the effects of different factors on the three algorithms.

Next, extensive measurement campaigns were conducted in different experimental settings to derive the path loss model and find the variation of the environment-specific parameters from environment to environment. These campaigns can be used to estimate the path loss characteristics of the sensor field prior to the deployment of the location finding systems or for the simulation of a sensor field for future experiments. The method used to model the path loss characteristics of a channel were described in detail. Since the algorithms are applied to RSS-based distance measurements, it compels us to learn more about the various factors that could cause anomalies in the ranging data.

Albeit, the performance of the algorithm is verified using RSS in this thesis, our algorithm can be applied to time of arrival (TOA) based distance estimates or time difference of arrival (TDOA) based distance estimates as well. The challenges of using RSS data for localization are discussed in detail in Chapter 6 of this thesis. An in-depth study of radio channel propagation characteristics reveals various factors which could affect the performance of a localization technique based on RSS.

A channel measurement based evaluation method is designed to compare the performances of algorithms individually. The localization experiment is performed in an indoor setting and the path loss model obtained from the measurement campaigns is used to convert the received signal power to distance estimates. The algorithm is then applied

to the data obtained from the experimental setup and the cumulative distance error is calculated.

1.6. Organization of the Thesis

The rest of the thesis is organized as follows. Chapter 2 concentrates on some of the work done in the area of localization in wireless sensor networks. It describes the existing location finding systems and discusses the framework of our localization system. Chapter 3 details a theoretical formulation of the maximum likelihood estimator (MLE) algorithms in Section 3.2 and multidimensional scaling (MDS) in Section 3. These algorithms are further integrated to produce the MDS-MLE algorithm in Section 3.3. After a description of the techniques used for localization in this thesis, Chapter 4 describes an extensive simulation study of the performance of all the three algorithms under similar environmental conditions. Section 4.2 studies the effect of the density of the sensor field on the performance of the algorithms. The effect of the density of the number of anchor nodes, which are nodes whose location coordinates are known apriori, is discussed in Section 4.3.

Chapter 5 lists the hardware and software used to implement the experimental testbed, followed by the features and functional details of the program implemented on the wireless sensor nodes. Chapter 6 discusses the experimental setup and the path loss modeling details. The radio channel characteristics are observed through extensive measurement campaigns in different settings. The localization experiment is setup in an indoor location and the received signal strength values are recorded for further experimental analysis. The experimental results are discussed in the same chapter followed by a study of various factors that could affect the performance of the location

estimation algorithms.

CHAPTER 2

LOCALIZATION IN WIRELESS SENSOR NETWORKS

Localization can be defined as a process of discovering the spatial relationships between different objects. It has emerged into a major research area in wireless sensor networks. It is a well established problem and several solutions have been proposed by researchers from varied disciplines like statistics, signal processing, computer science and systems engineering. A detailed overview of various location sensing technologies can be found in [11].

This chapter describes selected literature of the existing location finding systems in wireless sensor networks. This chapter also presents the technical aspects of the problem which will enable a sound understanding of the challenges involved in this domain. In the context of this thesis, the localization techniques are classified as traditional or non-collaborative localization techniques and collaborative localization techniques based on the nature of the method. Section 2.1 presents a study of the traditional methods of localization. Section 2.2 presents the details of collaborative localization techniques. Section 2.3 presents the challenges of developing a localization system for wireless sensor networks.

2.1. Traditional Localization Systems

Traditional localization approaches usually depend on some form of communication between reference nodes (nodes whose location information is known apriori) and location-unaware sensor nodes. These techniques do not require the location-unaware

sensor nodes to collaborate among themselves to estimate their location information. Such approaches are termed as non-collaborative localization techniques or traditional techniques, in the context of this thesis. In traditional techniques, the resolution of the solution is directly dependent upon the number of reference nodes used. In general, as the scale of the deployment is increases, the number of reference nodes necessary to determine the exact locations of the nodes also increases. Several of these localization techniques also require a sensor node to be present in the range of one or more reference nodes to be able to actually determine its location.

Localization techniques differ from each other in the method of obtaining distance estimates between sensor and reference nodes. Most of the localization techniques, both traditional and collaborative can be broadly classified into two categories: range-based or range-dependent schemes and range-free or range-independent schemes. Range-based schemes estimate distance based on timing, direction or radio signal strength [12-18]. The distance estimates used in these schemes are usually obtained from different methods like time of arrival (TOA), received signal strength (RSS), angle of arrival (AOA). Range-free localization methods do not need ranging data and can estimate the positions of sensor nodes based on connectivity or proximity information between nodes. Both kinds of techniques will be discussed in the following sections.

2.1.1. Time of Arrival (TOA)

Figure 2.1 shows a timing based method that infers distance between two nodes from the time of flight of a signal (RF, acoustic etc). This method is referred to as TOA or time of arrival. The product of the time delay between transmission and reception of a signal and its propagation velocity yields the separation distance between the transmitter and

receiver.

Time of arrival can also be calculated by making explicit time of flight measurements by propagating distinct signals with different propagation times, such as radio and acoustic signals (See Figure 2.2). Since these two signals travel at different speeds, the radio signal can be used to synchronize the sender and receiver and the acoustic signal can be used for ranging. This approach is referred to as time difference of arrival (TDOA) and is used for a higher precision.

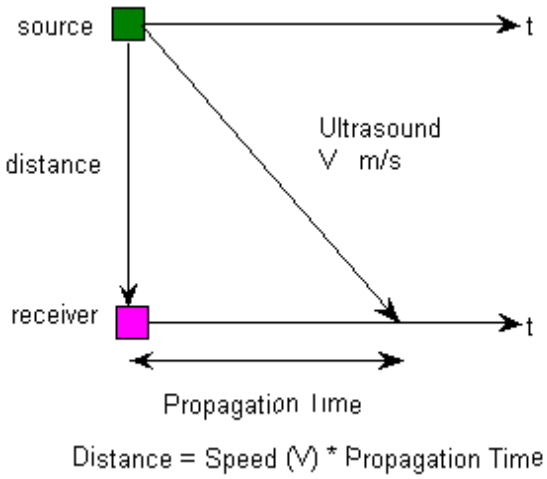

FIGURE 2.1. Time of Arrival. The time of flight of a signal is multiplied by the propagation speed of the signal in the medium to obtain the distance estimate of the receiver from the sender. Three such distance estimates from reference nodes can ensure location estimation through triangulation.

The most popular system to use TOA for localization is the GPS. Figure 2.3 shows trilateration in 2-dimensional geometric space. GPS uses trilateration extended to 3-dimensional space. Several localization techniques in wireless sensor networks, are based on some form of trilateration / multilateration techniques. TOA-based distance estimates

can be applied to trilateration to locate a sensor node. The minimum number of reference nodes required for a sensor node to exactly pin-point its location in trilateration is three, given the distance measures are error-free. However, TOA in wireless sensor networks is an expensive alternative since it demands additional hardware and is often very energy consuming.

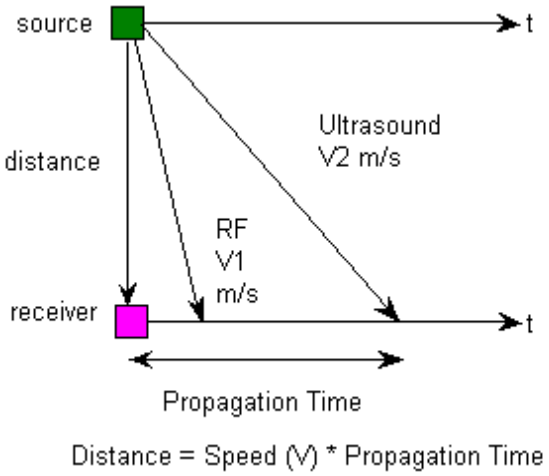

FIGURE 2.2. Time Difference of Arrival

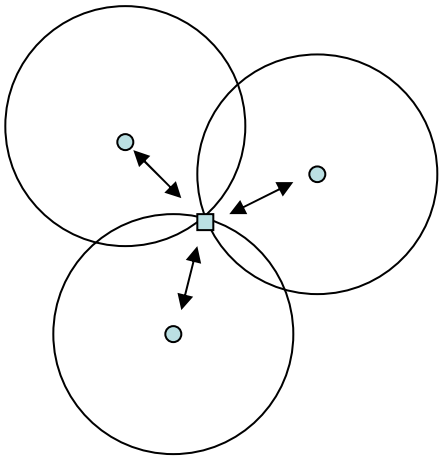

FIGURE 2.3. Triangulation. If the distance between the sensor node, represented by a square, and the reference nodes, represented as circles in the figure, is known, the location of the sensor node with respect to the reference nodes can be calculated geometrically.

2.1.2. Angle of Arrival (AOA)

In direction based ranging, the direction of each reference point with respect to the sensor node in some reference frame is used to determine the position of the sensor nodes (see Figure 2.4). The angle at which the signal is received is used to estimate the distance at which the sender node is located, using simple geometrical relationships. AOA is generally measured using directional antenna or antenna arrays.

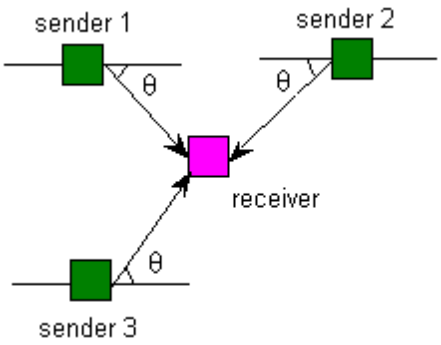

FIGURE 2.4. Angle of Arrival. The reference nodes measure the direction of arrival of a message from the location-unaware sensor node. Accurate arrival direction information from at least two reference nodes will give the position of the location-unaware node.

AOA in conjunction with TDOA allows nodes to estimate and map relative angles between neighbors. In general, the accuracy of the AOA estimation largely depends upon the radio propagation environments.

2.1.3. Received Signal Strength (RSS)

Communication between sensor nodes is via radio signals. Received Signal Strength is a measure of the power of a signal or message received at a receiver. In wireless sensor networks, the RSS parameter can be easily measured and requires no special hardware

implementation as almost all types of sensor nodes are equipped with received signal strength indicator (RSSI) circuits. The received signal strength measurements of a message can be used in two different ways to predict the location of a node: 1) Localization using RSS-based distance measurements and 2) Localization using signal pattern matching.

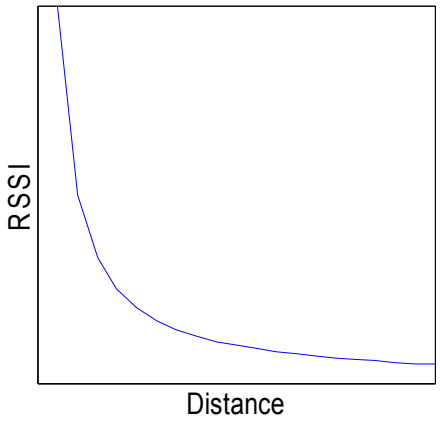

FIGURE 2.5. RSSI vs Distance. The average received signal strength decreases logarithmically over distance in near ideal environment.

Localization using RSS-based Distance Measurements

As an RF signal propagates in a medium from a transmitter to a receiver, the signal attenuates at a rate proportional to the distance traveled. (An approximation of the radio signal strength behavior in near-ideal medium can be seen in Figure 2.5) Usually, theoretical or empirical models are used to convert the signal strength into distance estimates. Path loss models portray the signal power attenuation level as the signal travels from transmitter to the receiver. If the path loss model of an environment is available either through prior assumptions or through experimental analysis, the distance between the receiver and transmitter can be calculated from the received signal strength of a

message received by the receiver. RSS measurements are usually inaccurate and error-prone, since they are affected by many factors such as multipath shadowing, interference and fading. However, due to their ease of accessibility researchers are finding ways to reduce the environment-dependent errors.

Distance measures obtained from path loss models are applied to techniques like triangulation for location estimation. RSS-based distance measures were used in several techniques such as in [12]. The SpotOn [12] ad-hoc location sensing system was used to track equipment and people. The SpotOn hardware tags which serve as object-location tags use the received signal strength information to estimate the inter-tag distance. They present a distance-dependent RSSI prediction function used to estimate distances from observed RSS values. This paper also presents calibration of the SpotOn radios to handle the hardware variability and improve the estimate accuracy. DV-distance propagation method in [16] also uses RSS values to measure the distance between sensor nodes. This thesis uses RSS-based distance estimates but in a collaborative fashion as will be seen shortly.

Localization using Signal Pattern Matching

Signal pattern matching is based on the assumption that, each grid or tile of a sensor field yields a unique fingerprint. Assuming there are n access points, each location-unaware sensor node measures the received signal strength from each of the access points and records them as a tuple. These tuples generate a fingerprint which is cross-checked with a signal signature database to match a grid or tile in the sensor field. However, substantial effort is consumed in creating the database initially through experimental

means. This system is not appropriate for ad hoc network scenarios and needs careful and precise signature collection and demands an expensive implementation.

RADAR [13], an RF-based system for locating and tracking users inside buildings using the IEEE 802.11 WaveLAN wireless networking technology, was presented by a Microsoft Research Group. It uses scene matching which is a form of signal pattern matching. Base stations were equipped with wireless adapters that provided an overlapping area of coverage to track a wireless enabled mobile node. Received signal strength of the signals sent by the mobile node was used to compute the 2D position of the mobile node using scene analysis and lateration. A technique called nearest neighbor(s) in signal space (NNSS) was used to compare multiple locations and choose the best location that matches the observed signal strength.

Multipath fading, background interference and shadowing in real-world environments introduce error into the RSS measurements and make them less credible. Though RSS is prone to measurement errors it remains a popular choice for low-power location estimation due to its wide availability and inexpensive implementation. TOA and AOA are less suitable for localization techniques although they are more accurate than RSS, since they are energy-consuming and expensive.

2.1.4. Range-free Techniques

Range-free schemes do not need distance or angle information for localization. These methods usually rely on proximity or connectivity information obtained from the sensor network. In Active Badge system [19], each person or object is tagged with an Active Badge, which transmits a unique IR signal periodically to the sensors placed at fixed positions within the facility. These sensors relay the information to location management

software which provides information of the person's location to the requesting applications. This scheme however yields a coarse solution based on infrared (IR) technology and is only suitable for shorter ranges.

The Cricket Indoor Location System [20] also uses beacons attached to the ceiling of a building and receivers attached to devices whose location should be known. Each beacon periodically transmits an RF message containing its location information and an ultrasonic pulse, which when received by the listeners is used to calculate its distance from the beacon. Distance information obtained from all the beacons is used to find the location information. [21] uses a centroid based method to localize sensor nodes. This method requires beacons or reference nodes which know their locations, to send out periodic signals. The other nodes receive these signals and calculate the centroid of these beacons points. This approach relies on a large number of beacon nodes for higher accuracy.

DV-HOP proposed in the ad hoc positioning system (APS) [16] assumes a heterogeneous network consisting of sensing nodes and anchors. Instead of single hop broadcasts, anchors flood their location throughout the network maintaining a running hop-count at each node along the way. Nodes calculate their position based on the received anchor locations, the hop-count from the corresponding anchor, and the average-distance per hop; a value obtained through anchor communication.

2.2. Collaborative Localization Techniques

Collaborative localization techniques are a class of techniques which utilize distance measurements between pairs of location-unaware sensor nodes. Unlike traditional localization techniques, collaborative localization techniques exploit the ad-hoc

networking capabilities of all the sensor nodes instead of just the reference nodes, for location estimation. Collaborative location estimation algorithms allow location-unaware sensor nodes that are not in the range of any reference nodes to be located, provided they have at least one neighboring sensor node. Such algorithms do not demand an overlapping coverage of reference nodes and work well in sparse reference node configurations. Generally, they yield more accurate results due to the availability of greater resolution of data to estimate a sensor node location.

Savvides et al [22] proposed AHLoS (ad hoc localization system), which uses beacon nodes (nodes whose position is known apriori) for a location discovery process called iterative multilateration. Atomic multilateration is used to propagate the process of iterative multilateration by starting location estimation using minimum mean square estimation with an unknown node (node whose location information is unknown) which is within the range of at least three beacon nodes. The beacon nodes broadcast their location information to the sensor network. Nodes which receive the broadcast measure their separation from their neighbors and use the beacon messages to estimate their own positions. Once a node knows its position, it starts behaving like a beacon node itself and propagates the beacon message. This process is repeated until all the nodes collaboratively discover their positions. AHLoS was implemented using both RSS-based distance measures and TDOA-based (RF and Ultrasound signals used for synchronization and ranging respectively) distance measures. However, it can be observed that iterative multilateration accumulates error and requires relatively high percentage of beacon nodes. With a good ranging method, the algorithm can produce accurate position estimates.

Shang et al. proposed MDS-MAP [23] which uses connectivity information to obtain location information of the nodes in a sensor network. The technique is based on classical multidimensional scaling (MDS), a technique used to convert data proximity information to geometric embedding. They present two methods based on MDS: MDS-MAP(C), which builds the network map using classical MDS and MDS-MAP(P), which builds local maps and stitches them together to form a global map. MDS-MAP(P) achieves better results in irregular networks. It operates by setting the number of hops as range for local maps and applies MDS-MAP(C) within this range to generate its local map. These maps are stitched together by choosing local maps which share the maximum number of neighbor nodes with the current map. MDS-MAP method works fine with connectivity information as well as range measurements to produce absolute maps or relative maps in the case of the absence of reference nodes.

Costa et al. proposed the distributed multidimensional scaling with adaptive weighting algorithm [24] which can be applied to RSS or TOA ranging data. This is a distributed algorithm where each sensor node chooses a neighborhood of sensors and computes its position estimate by minimizing a cost function through majorization and then passes this position update to its neighbors. Further, the inhomogeneous character of range measurements is taken care of by applying weights to measurements which are believed to be more accurate.

Patwari et al. [8] propose a relative location estimation method for self-configuration of sensor nodes through the measurement of time of arrival and received signal strength between all the neighbors of a sensor node. A small fraction of nodes called reference nodes know their location information apriori. Cramer-Rao bound and

maximum likelihood estimator are derived under Gaussian model of TOA and log-normal model of RSS and are applied to measurements obtained from a wireless sensor network testbed.

It can be observed that collaborative techniques tend to reduce the error induced in distance estimates through collection of multiple distance measures. Since a sensor node communicates with multiple nodes, an error in its position estimate due to a noisy measurement reported by a neighboring node is automatically reduced by the other neighbors.

2.3. Challenges in the Design of Sensor Localization Techniques

A low-power sensor network demands a low complexity localization solution. Low energy consuming devices contribute to the longevity of a sensor network. Though ranging techniques like AOA and TOA provide accurate distance estimates, they require additional energy-consuming hardware making them an expensive alternative. RSS appears to be a wise choice for an energy-intensive sensor network since almost all types of sensor nodes have a built-in received signal strength indicator (RSSI) circuit for RSS measurement.

Low-power sensor nodes are not capable of long range communication. In traditional localization techniques, every sensor node has to be within the communication range of at least one or more reference nodes to localize it. For a large-scale deployment, this arrangement can get quite cumbersome and unrealistic. Location estimation techniques should allow localization even in the absence of a reference node in the vicinity of a sensor node. This is possible through collaborative localization techniques.

Though, collaborative algorithms tend to be more efficient than traditional algorithms, the source of error in both the techniques arises from the ranging model employed. The impact of the RSS metrics on the performance of the algorithm is significant and motivates researchers to look for efficient ways to reduce the effect of these errors. Though RSS provides an inaccurate estimate of the distance measurements, collaborative ranging subdues the effect of noise in the measurements. Problems such as multi-path fading, background interference and irregular signal propagation make range measurements inaccurate. Several methods such as robust range estimation [25], parameter calibration [26], [27] and two-phase refinement positioning [28] have been proposed to take advantage of averaging and smoothing to mitigate the errors in measurements to a certain extent.

CHAPTER 3

COLLABORATIVE LOCALIZATION METHODS

A resource-constrained wireless sensor network demands a low-complexity solution for localization, and an RSS-based location estimation system appears to be a good choice due to its wide availability and low cost. This chapter concentrates on RSS-based localization systems designed to collaboratively estimate sensor node positions through the accumulated received signal strength. Multidimensional Scaling (MDS) and Maximum Likelihood Estimation (MLE) are two such algorithms which use RSS ranging data based distance estimates to localize sensor nodes. An analysis of these two algorithms via formulation shows that MLE is asymptotically efficient due to an assumption of log-normal shadow fading effects and that MDS has a very good convergence property. Similar findings incited a synthesis of these two algorithms resulting in a new algorithm called, MDS-MLE which exploits the positive features of the algorithms and automatically eliminates problems inherent in the implementation of the two techniques.

3.1. RSS-based Ranging

Collaborative localization algorithms which employ pair-wise distance measurements based on the received signal strength parameter require an efficient power to distance transformation function which accounts for environment-specific errors. This section presents the path loss model which is used to predict the distance from the received signal

strength measurements.

Unlike the free-space model, which assumes that the communication range is an ideal circle, path loss model takes into account the multipath propagation effects. Path loss occurs due to the decay of the intensity of a propagating radio wave. The received power of a signal transmitted from node i to node j, at a distance d_{ij} is denoted as $\overline{P_{ij}}$, and decays at a rate proportional to $d^{-\alpha}$, where α represents the path loss exponent ($\alpha = 2$ for ideal free-space channel model). A close-in distance d_0 is used as a reference distance and the received power at distance d_0 represented as $\overline{P_0}$ are used to compute the distance corresponding to a received power.

(3.1) $$\frac{\overline{P_0}}{\overline{P_{ij}}} = \left(\frac{d_{ij}}{d_0} \right)^{\alpha}.$$

The value of the path loss exponent increases as the obstructions in a field increase, hence, the received power falls at a faster rate as the distance increases. Path loss is usually measured in dBm, hence (3.1) is transformed to

(3.2) $$P_{ij} = P_0 - 10\alpha \log_{10} d_{ij} - v_{ij},$$

where P_0 is the received power in dBm unit at a distance of $1\,\mathrm{m}$, d_{ij} is the distance between node i and node j, P_{ij} is the received power in dBm measured at node j (transmitted by node i) and v is a Gaussian random variable representing log-normal shadow fading effects in complex multipath environments [29]. In the literature of radio propagation channel studies, the random variable v is considered zero-mean, that is,

$v \sim N(0, \sigma_v^2)$, while the value of the standard deviation σ_v depends on the characteristics of a specific multipath environment.

The parameters of the path loss model are decided after analyzing the RSS-based experimental ranging data as will be shown in Chapter 6. These parameters can be further used to produce simulations which mimic an environment.

3.2. Maximum Likelihood Estimator

Maximum Likelihood Estimator or MLE can be implemented for any data whose statistical model is known. Many years of study of radio propagation models has asserted that the variation of the received signal power at a certain distance is best described by a log-normal random variable. It follows Gaussian distribution, if the power is measured in dB. This is supported by several studies based on radio channel measurement and has been tested through experimental study in wireless sensor networks [30], [32]. Since, the shadow fading effects are assumed to be log-normal; MLE appears to be a natural choice of estimator. The principle of maximum likelihood estimator was originally developed by R.A.Fisher [33] and states that the desired probability distribution is one that makes the observed data "most likely" [34]. MLE has been used widely due to its ease of computation and its asymptotic optimality properties which make it very consistent and efficient. The maximum likelihood estimator determines the one probability distribution function (PDF) from a set of PDFs the model describes, which is most likely to have produced the data, when the observed data and a model of interest are given. That is, if $p(x \mid \theta)$ denotes the probability density function that specifies the probability of observing data x given the parameter θ, $L(\theta \mid x)$ represents the maximum likelihood

estimator is the likelihood of a parameter given the observed data x [34]. $L(\theta \mid x)$ can be given by,

$$L(\theta \mid x) = p(x \mid \theta).$$

It can be easily derived from (3.2) that the maximum likelihood estimator (MLE), based on RSS measurement of the distance [8] between node i and node j is,

$$\delta_{ij} = 10^{(P_0 - P_{ij})/(10\alpha)} . \tag{3.3}$$

Assume a sensor network which consists of N_1 sensor nodes with unknown location coordinates and N_2 reference nodes with known location coordinates. Without loss of generality, here we define $N = N_1 + N_2$. The location coordinates of N nodes in the M-dimensional space are grouped into an $N \times M$ configuration matrix

$$\mathbf{X} = [\mathbf{r}_1 \quad \mathbf{r}_2 \quad ... \quad \mathbf{r}_N]^T ,$$

where $\mathbf{r}_i = [x_{i1} \quad x_{i2} \quad ... \quad x_{iM}]^T$ are the location coordinates of node i. $\mathbf{X}$ represents the sensor node configuration estimated using MLE. For the ease of derivation that follows, here we define that $\mathbf{r}_i$, $1 \le i \le N_1$, are unknown location coordinates of sensor nodes while $\mathbf{r}_i$, $N_1 + 1 \le i \le N$, are known location coordinates of reference nodes. The original distance/dissimilarity collected from the sensor network deployment is δ_{ij} and forms an $N \times N$ symmetric matrix. If the collected distance measurements are error-free, δ_{ij} and $d_{ij}(\mathbf{Z})$ will be equal. In reality, δ_{ij} can have missing distance measurements. To account for this, an $N \times N$ weight matrix is defined with fixed weights $w_{ij} = 1$ if δ_{ij} is known and

$w_{ij} = 0$ if δ_{ij} is missing.

For RSS-based collaborative localization, the MLE of the configuration matrix $\mathbf{X}$ can be derived by minimizing the cost function,

$$S_{ML}(\mathbf{X}) = \sum_{i=1}^{N-1} \sum_{j=i+1}^{N} w_{ij} (\ln d_{ij}(\mathbf{X}) - \ln \delta_{ij})^2 , \tag{3.4}$$

where $S_{ML}(\mathbf{X})$ is the cost function to be minimized. For 2-D localization, (3.4) can be rewritten as

$$S_{ML}(\boldsymbol{\theta}) = \sum_{i=1}^{N_1} \sum_{j=i+1}^{N} w_{ij} (\ln d_{ij}(\boldsymbol{\theta}) - \ln \delta_{ij})^2 , \tag{3.5}$$

where $\boldsymbol{\theta} = [\boldsymbol{\theta}_x^T \quad \boldsymbol{\theta}_y^T]^T$ while $\boldsymbol{\theta}_x$ and $\boldsymbol{\theta}_y$ are column vectors of the unknown x and y coordinates of all sensor nodes, respectively. The minimization problem in (3.6) can be solved with iterative numerical optimization algorithms such as the trust-region method implemented in Matlab [48].

MLE is asymptotically efficient due to the assumption of log-normal shadow fading effects. However, MLE is sensitive to local maxima, i.e., unless it is initialized to a start configuration which is close to the original configuration, MLE may stop prematurely and yield sub-optimal parameters. One of the ways to ensure a global optimum is reached is to choose different start configurations over several runs of the algorithm and check if the solution obtained is constant. The next section presents another collaborative localization algorithm based on RSS measurements called multidimensional scaling (MDS).

3.3. Multidimensional Scaling

Multidimensional scaling (MDS) belongs to a category of multivariate data analysis methods which are used to provide a visual representation of the pattern of dissimilarities, or distances in this case, among a set of objects. Torgerson proposed one of the first well-known MDS techniques in 1952 [35]. Though MDS has its origins in psychophysics and psychometrics, it has been used in a range of fields including political science, psychology, anthropology, economics, education and behavioral, econometric, and social sciences [36]. MDS is very appropriate for the node localization problem, where the location coordinates of the sensor nodes can be obtained from distance based dissimilarities. MDS is used to discover spatial structures in data and model them in the geometric space. There are many kinds of MDS. Metric MDS which is a superset of classical MDS is used in this thesis. Metric MDS is used for quantitative data. It finds a configuration of points in some multidimensional space such that the inter-point distances are related to the experimentally obtained dissimilarities by a transformation function [37]. MDS can be used either to produce a relative map which shows how the sensor nodes are aligned with respect to each other or to produce an absolute map which shows the absolute location coordinates of the sensor nodes in 2-dimensional or 3-dimensional space. The relative map might suffice for applications like geographic routing algorithms [5], [6]. However, it might not be very useful for other applications like target tracking which require the absolute location of an event. The absolute map can be generated from the relative map, if the original coordinates of a few sensor nodes, generally referred to as the reference or anchor nodes, are known apriori.

MDS can be seen as a method which involves rearranging objects in the fashion which best portrays the observed distances. MDS starts with an initial sensor location configuration and refines it until a specified threshold of error is reached. The collaborative localization in sensor networks is formulated into an MDS problem in the following sections.

3.3.1. Stress Function

$\mathbf{Z}$ represents the original configuration matrix of the sensor nodes and contains location coordinates of N nodes in the M-dimensional space grouped into an $N \times M$ matrix,

$$\mathbf{Z} = [\mathbf{r}_1 \quad \mathbf{r}_2 \quad ... \quad \mathbf{r}_N]^T,$$

where $\mathbf{r}_i = [z_{i1} \quad z_{i2} \quad \ldots z_{iM}]$ are the location coordinates of node i. $d_{ij}(\mathbf{Z})$ represents the distance between sensor nodes i and j based on their position in $\mathbf{Z}$.

(3.6) $$d_{ij}(\mathbf{Z}) = \| \mathbf{r}_i - \mathbf{r}_j \| = (\sum_{a=1}^{m} (z_{ia} - z_{ja})^2)^{\frac{1}{2}}.$$

$\mathbf{X}$ represents an $N \times M$ matrix of the estimated location coordinates of the sensor nodes. $d_{ij}(\mathbf{X})$ represents the distance between sensor nodes i and j based on their estimated positions in $\mathbf{X}$ and

(3.7) $$d_{ij}(\mathbf{X}) = (\sum_{a=1}^{m} (x_{ia} - x_{ja})^2)^{\frac{1}{2}} \quad .$$

A *Stress* function is computed that measures the difference of the distances between the estimated locations $\mathbf{X}$ in the geometric space ($d_{ij}(\mathbf{X})$) and the corresponding

dissimilarities obtained from the configuration matrix $\mathbf{Z}(\delta_{ij})$ [38]. $\mathbf{X}$ is approximated to find the location matrix by minimizing this Stress function, $S_r(\mathbf{X})$,

$$S_r(\mathbf{X}) = \sum_{i=1}^{N-1} \sum_{j=i+1}^{N} w_{ij} (d_{ij}(\mathbf{X}) - \delta_{ij})^2 \ . \tag{3.8}$$

$\mathbf{X}$ is initialized with a random $N \times M$ coordinate matrix as $\mathbf{X}^{[0]}$ in the beginning and is updated to $\mathbf{X}^{[1]}, \mathbf{X}^{[2]}, \mathbf{X}^{[3]} \ldots\ldots$ with every iteration, either until the maximum number of iterations is reached or until the difference between the values of *Stress* function of two consecutive iterations falls below a preset empirical threshold, ε.

3.3.2. SMACOF

This Stress has to be minimized so that the result can get as close as possible to the original configuration. To find the minimum of a function, it is not always possible to differentiate the function, equating it to zero and solving for the variable. We use a method called iterative majorization, which improves the position estimate by using the output from the previous estimate as an input for the next set of computations [38]. It generates a monotonically non-increasing sequence of function values. The majorization algorithm used in this thesis to minimize the Stress function is SMACOF. SMACOF initially stood for "Scaling by Maximizing a Convex Function", but later on came to be known as "Scaling by Majorizing a Complicated Function" [38].

Expanding the Stress function from (3.7) results in

$$S_r(\mathbf{X}) = \sum_{i=1}^{N-1} \sum_{j=i+1}^{N} w_{ij} (d_{ij}(\mathbf{X}) - \delta_{ij})^2 \ ,$$

$$S_r(\mathbf{X}) = \sum_{i=1}^{N-1}\sum_{j=i+1}^{N} w_{ij} d^2{}_{ij}(\mathbf{X}) + \sum_{i=1}^{N-1}\sum_{j=i+1}^{N} w_{ij}\delta^2{}_{ij} - \sum_{i=1}^{N-1}\sum_{j=i+1}^{N} w_{ij} d_{ij}(\mathbf{X})\delta_{ij} ,$$

$$S_r(\mathbf{X}) = \eta^2(\mathbf{X}) + \eta_\delta^2 - 2\rho(\mathbf{X}). \tag{3.9}$$

Upon decomposing the expression, the Stress function yields three parts. The second term in the equation, η_δ^2, depends on the dissimilarity matrix, δ_{ij} and the weight matrix w_{ij}, which is obtained from the dissimilarity matrix. The first term $\eta^2(\mathbf{X})$, is a sum of products of weight matrix and squared distances of X. The Euclidean distance between a pair of sensor nodes can be written as

$$d_{ij}{}^2(\mathbf{X}) = tr\,\mathbf{X}'\mathbf{A}_{ij}\mathbf{X}, \tag{3.10}$$

where $\mathbf{A}_{ij}$ is a matrix with $a_{ii} = a_{jj} = 1, a_{ij} = a_{ji} = -1,$ and all the other elements zero. $\mathbf{A}_{ij}$ is row and column centered, so that $\mathbf{A}_{ij}1 = 0$ and $1'\mathbf{A}_{ij} = 0'$. Each term of $\eta^2(\mathbf{X})$ is

$$w_{ij} d^2{}_{ij}(\mathbf{X}) = w_{ij}\ tr\,\mathbf{X}'\mathbf{A}_{ij}\mathbf{X} = tr\ \mathbf{X}'(w_{ij}\mathbf{A}_{ij})\mathbf{X}. \tag{3.11}$$

Adding all these terms amounts to

$$\eta^2(\mathbf{X}) = \sum_{i=1}^{N-1}\sum_{j=i+1}^{N} w_{ij} d^2{}_{ij}(\mathbf{X}) = tr\,\mathbf{X}'\left(\sum_{i=1}^{N-1}\sum_{j=i+1}^{N} w_{ij}\mathbf{A}_{ij}\right)\mathbf{X} = \mathrm{tr}\,\mathbf{X}'V\,\mathbf{X}. \tag{3.12}$$

Basically, $v_{ij} = -w_{ij}$ if $i \neq j$ and $v_{ii} = \sum_{j=1}^{n} - w_{ij}$, for the diagonal elements of,

$$V = \sum_{i=1}^{N-1}\sum_{j=i+1}^{N} w_{ij} A_{ij} .$$

The third term of the decomposed Stress function is simplified by obtaining a majorizing inequality for $-d_{ij}(\mathbf{X})$ using the Cauchy-Schwarz inequality [38],

$$-\rho(\mathbf{X}) = -\sum_{i=1}^{N-1}\sum_{j=i+1}^{N} w_{ij}\delta_{ij}d_{ij}(\mathbf{X}),$$

$$\leq \text{tr } \mathbf{X}'\left(\frac{w_{ij}\delta_{ij}}{d_{ij}(\mathbf{Z})}\mathbf{A}_{ij}\right)\mathbf{Z},$$

$$= \text{tr } \mathbf{X}'\mathrm{B}(\mathbf{Z})\mathbf{Z},$$

where $\mathrm{B}(\mathbf{Z})$ has elements,

$$b_{ij} = \begin{cases} \frac{w_{ij}\delta_{ij}}{d_{ij}(\mathbf{Z})} & \text{for } i \neq j \text{ and } d_{ij}(\mathbf{Z}) \neq 0 \\ 0 & \text{for } i \neq j \text{ and } d_{ij}(\mathbf{Z}) = 0 \end{cases},$$

$$b_{ij} = -\sum_{j=1, j\neq i}^{n} b_{ij}.$$

Since equality is achieved when $\mathbf{Z} = \mathbf{X}$,

$$-\rho(\mathbf{X}) = \text{tr } \mathbf{X}'\mathrm{B}(\mathbf{X})\mathbf{X} \leq \text{tr } \mathbf{X}'\mathrm{B}(\mathbf{Z})\mathbf{Z}. \tag{3.13}$$

Substituting (3.12) and (3.13) in (3.9), the Stress function is updated as,

$$\begin{aligned} S_r(\mathbf{X}) &= tr\ \mathbf{X}'V\mathbf{X} + \eta_\delta^2 - \text{tr } X'B(\mathbf{X})\mathbf{X} \\ &\leq tr\ \mathbf{X}'V\mathbf{X} + \eta_\delta^2 - \text{tr } X'B(\mathbf{Z})\mathbf{Z} \end{aligned} \tag{3.14}$$

A minimum of this function can be obtained by setting the derivative to zero and solving for **X**.

$$\mathbf{X} = V^{-1}B(\mathbf{Z})\mathbf{Z} \tag{3.15}$$

V is not of full rank, so the Moore-Penrose inverse of V is used instead. The Moore-Penrose inverse of V represented as V^{+} is given by

(3.16) $$V^{+} = (V + 11^{'})^{-1} - n^{-2}11^{'}.$$

(3.15) is updated using (3.16) as,

(3.17) $$\mathbf{X}^{p} = V^{+} B(\mathbf{Z})\,\mathbf{Z}.$$

This is called the Guttman transform [38] and is simplified to (3.18) if all the distance measurements are present, i.e., when all $w_{ij} = 1$.

(3.18) $$\mathbf{X}^{p} = n^{-1} B(\mathbf{Z})\,\mathbf{Z}.$$

The algorithm to obtain relative configuration of a sensor network from a random initial configuration matrix $\mathbf{X}^{[0]}$ follows:

- Step 1: Initialize $\mathbf{Z}$ with $\mathbf{X}^{[0]}$ and set the iteration counter, k to zero.
- Step 2: Compute the Stress function, $S_r(\mathbf{X}^{[0]})$ for $\mathbf{X}^{[0]}$.
- Step 3: Increment the counter, k by one.
- Step 4: Compute $\mathbf{X}^{[k]}$ through Guttman transform (3.17) or (3.18).
- Step 5: Compute $S_r(\mathbf{X}^{[k]})$.
- Step 6: Compare $(S_r(\mathbf{X}^{[k]}) - S_r(\mathbf{X}^{[k-1]})$ with ε. Stop if the difference is smaller than ε. Stop if the iteration counter reaches a maximum limit. Continue otherwise.
- Step 7: Set $\mathbf{Z} = \mathbf{X}^{[k]}$ and continue to Step 3.

The value of the *Stress* function is calculated in every step and compared with the value in the previous iteration. This process is repeated until the difference in the *Stress* value between two successive iterations leads to a value smaller than ε,

$$S_r(\mathbf{X}^{[k]}) - S_r(\mathbf{X}^{[k-1]}) < \varepsilon .$$

ε, an empirical threshold based on the accuracy requirement is decided based on the accuracy requirement. It is kept low in most cases to allow for greater accuracy.

This method yields relative positions of the sensor nodes based on the distance information obtained from the network. The next section deals with position alignment techniques which use the knowledge of locations of the reference nodes to update these relative coordinates to geographical coordinates

3.3.3. Procrustes Similarity Transforms

The configuration of the sensor node locations obtained from the SMACOF transform has to be transformed further to match the orientation of the physical deployment. The problem of matching a configuration to another as nearly as possible can be regarded as the Procrustes problem [38]. In this context, the coordinates of the reference nodes obtained from the SMACOF transform are rotated to fit the original physical coordinates. $\mathbf{X}^{[k]}$, the final estimate obtained from SMACOF is denoted as $\mathbf{X}$ for clarity purposes. $\mathbf{X}_r$ represents the estimated reference node coordinates obtained from $\mathbf{X}^{[k]}$. $\mathbf{Y}$ represents the $((\mathbf{N} - \mathbf{N_1}) \times \mathbf{M})$ matrix of original coordinates of the reference nodes known apriori. The order of $\mathbf{X}_r$ and $\mathbf{Y}$ matrices is the same.

A measure of the closeness, of the two configurations $\mathbf{X}_r$ and $\mathbf{Y}$ is obtained by calculating the sum of squares of distances between corresponding points in both the configurations. This sum denoted as $\mathbf{L}$, has to be minimized by choosing an appropriate transformation matrix, $\mathbf{T}$.

(3.19) $$\mathbf{Y} \approx \mathbf{X_r T}\,.$$

L is obtained from the main diagonal of the product matrix of $\mathbf{(Y - X_r T)(Y - X_r T)'}$ as

(3.20) $$L(\mathbf{T}) = tr\ \mathbf{(Y - X_r T)(Y - X_r T)'},$$

$$= tr\ \mathbf{Y'Y} + tr\ \mathbf{T'X_r'X_r T} - \mathbf{2}tr\mathbf{Y'X_r T}\ ,$$

$$= tr\ \mathbf{Y'Y} + tr\ \mathbf{X_r'X_r} - \mathbf{2}tr\mathbf{Y'X_r T}\,.$$

Since, $tr\ \mathbf{Y'Y}$ and $tr\ \mathbf{X_r'X_r}$ are not dependent on $\mathbf{T}$, $L(\mathbf{T})$ can be minimized after it is reduced to

(3.21) $$L(\mathbf{T}) = c - 2tr\,\mathbf{Y'X_r T},$$

where c is a constant, not dependent on $\mathbf{T}$.

If $\mathbf{P'P = I}$ and $\mathbf{Q'Q = I}$, and $\mathbf{P\Phi\Phi'}$ is the singular value decomposition(SVD) of $\mathbf{Y'X_r}$, applying the invariance of the trace function under cyclic permutation and Kristof's inequality to (3.21), gives

$$L(\mathbf{T}) = c - 2tr\,\mathbf{Y'X_r T} = c - 2tr\ \mathbf{P\Phi\Phi'T},$$

(3.22) $$= c - 2tr\,\mathbf{Q'TP\Phi}\,.$$

If $\mathbf{T}$ is orthonormal, so is $\mathbf{Q'TP}$ and Kristof's inequality shows that the minimum of $L(\mathbf{T})$ is reached whenever $\mathbf{Q'TP = I}$ which implies that $\mathbf{T}$ should be chosen as

(3.23) $$\mathbf{T = QP'}\,.$$

The optimum rotational matrix $\mathbf{T}$ is obtained from a product of $\mathbf{Q}$ and $\mathbf{P'}$. $\mathbf{Q}$ and $\mathbf{P}$ are obtained by computing the SVD of $\mathbf{X'JY}$, where $\mathbf{J}$ is the centering matrix

$\mathbf{I} - n^{-1}\mathbf{1}\mathbf{1}'$. The translation vector, $\mathbf{t}$ is obtained as,

(3.24) $$\mathbf{t} = n^{-1}(\mathbf{X}_r - s\mathbf{Y}\mathbf{T})'1.$$

The matrix $\mathbf{X}$ is transformed to the final solution $\mathbf{X_f}$, by substituting the values of the rotational and translational factors $\mathbf{T}$ and $\mathbf{t}$ obtained from (3.23) and (3.24) as,

(3.25) $$\mathbf{X_f} = \mathbf{X}\mathbf{T} + 1\mathbf{t}'.$$

The sensor configuration obtained after SMACOF and Procrustean transformations is not close enough to the original solution in many cases. This solution can be refined by making the algorithm iterative. The estimate improves with every iteration, since the algorithm starts with an initial configuration which is closer to the original configuration. The algorithm can be stopped when the resultant configuration does not show any improvement over the previous solution. Another option is to set the iteration counter to a value decided before hand.

The algorithm can be summarized as:

- Step 1: Initialize $\mathbf{Z}$ with $\mathbf{X}^{[0]}$ and set the iteration counter, k to zero.
- Step 2: Perform SMACOF transform on $\mathbf{Z}$. Set $\mathbf{Z} = \mathbf{X}^{[k]}$, where $\mathbf{X}^{[k]}$ is the final result.
- Step 3: Perform Procrustes transformation on $\mathbf{Z}$. Set $\mathbf{Z} = \mathbf{X_f}$, where $\mathbf{X_f}$ is the transformed matrix.
- Step 4: Stop if the iteration counter k reaches the maximum. Otherwise, increment the counter and go to Step 2.

In our algorithm, we choose three different start configurations and select the

optimum result of the three. This will eliminate the scenarios where a poor start configuration might lead to a poor result, to a certain extent.

Unlike traditional localization systems, MDS does not require a sensor node to be in the range of a reference node to accurately estimate its position. All the sensor nodes communicate with their neighboring sensor nodes and use this information to find its relative location among the sensor nodes. Multidimensional Scaling is performed on the distance estimates obtained from the received signal strength values collected from the sensor network. Though the algorithm has a complexity of $O(N^3)$, it is not resource-consuming since it is computed on a centralized system. The performance of MDS degrades as the number of missing pair-wise distance measurements increase.

3.4. MDS - MLE

It can be observed from the above formulations that, MLE tends to work well when the data is modeled as a log-normal distribution. RSS measurements have been observed to have log-normal errors due to shadowing. This makes MLE a good candidate for location finding systems based on received signal strength. However, from the simulation results shown in the next chapter, it is seen that MLE is more sensitive to initial estimate than the SMACOF majorization algorithm used in MDS, i.e., it is not likely to reach the global maximum with a poor initial configuration.

MDS has inherent modeling errors due to which, though it produces a good estimate it is not close enough to the original configuration. MDS produces a coarse estimate which can be used as the initial start configuration for MLE. An integration of these two techniques in series will take advantage of the convergence property of MDS and will

enable MLE to produce a near-optimal estimate by fine-tuning the solution produced by MDS. This algorithm called MDS-MLE was observed to perform well under simulation settings as seen in the next chapter.

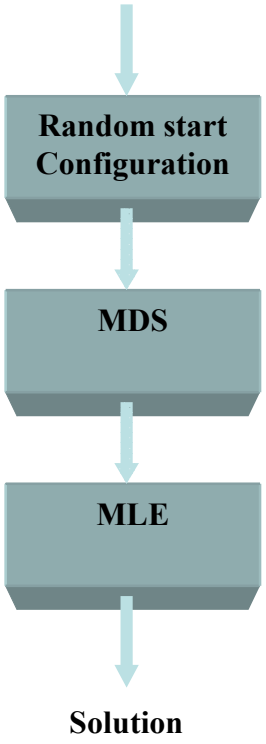

FIGURE 3.1. Block diagram of the MDS-MLE algorithm

Figure 3.1 shows the flow of the MDS-MLE algorithm. The MDS-MLE solution avoids the local minima problem inherent to MLE, by providing it a rough estimate of the original locations of the sensor nodes as the initial configuration. The MDS-MLE solution is obtained after the estimates are refined individually by MDS and MLE, in order to improve the solution by using the result of an iteration as the input to the succeeding set of iterations. Simulation studies in Chapter 4 show that MDS-MLE

consistently outperforms MDS and MLE.

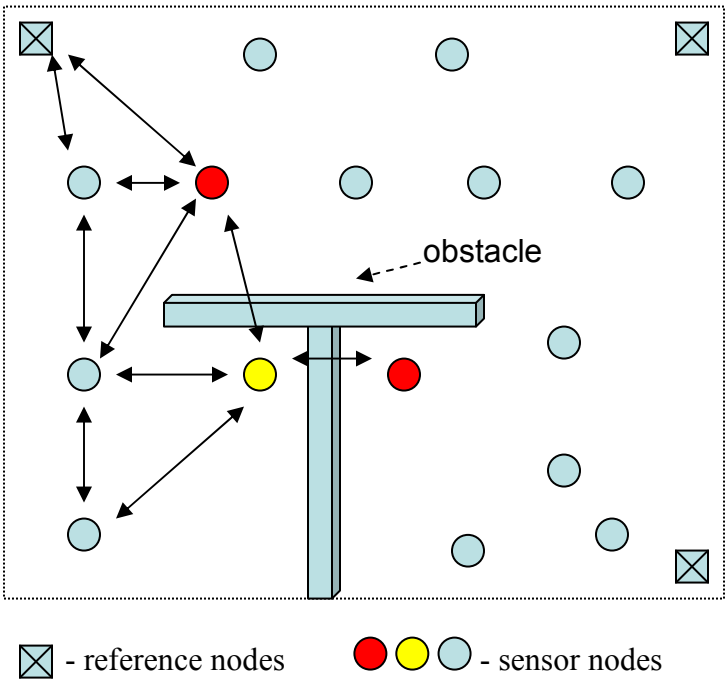

FIGURE 3.2. An example of collaborative location discovery. The sensor nodes shown as ⊠ act as the reference nodes. The error in location estimate produced due to noisy distance measurements between sensor node represented by ● and sensor nodes represented by ● due to a non-line of sight condition is mitigated by the distance measurements obtained from the other neighbors in the line of sight of the node.

Another major concern in location estimation is a no line of sight scenario. Such scenarios are encountered very often and pose as a major problem due to the errors induced in the distance measurements. Collaborative techniques can reduce the effect of such conditions due to the presence of multiple measurements from several sources.

Figure 3.2 shows such a scenario where the sensor node colored yellow, is surrounded by a wall. The directional arrows represent the communication links between sensor nodes. Pair-wise distance measurements between the said sensor node and the nodes colored in red are not precise due to the presence of obstacles. However, the effect of this error is mitigated by the measurements recorded by the other sensor nodes which are in its line of sight. It should also be noted that collaborative localization systems can indirectly localize a sensor node through its neighbors, even if it is out of the communication range of all the reference nodes. This eliminates the need to check if the reference nodes have an overlapping area of coverage.

3.5. Summary

Collaborative localization algorithms offer a good estimate of a sensor node's position even if the sensor node is not within the range of at least a single reference node. The purpose of the collaborative localization in sensor network is to estimate the unknown location coordinates of sensor nodes based on the pair-wise distance measurements of reference nodes and the other location-unaware sensor nodes. Traditional non-collaborative localization systems need three or more reference nodes to pin-point a sensor node location as shown in Chapter 2. RSS based localization systems are favored over other localization systems because RSS enabled wireless sensor nodes are widely available. However, MDS, MLE and MDS-MLE formulated for RSS-based ranging data in this chapter can work equally well with TOA-based distance measurements. Nevertheless, the conversion of the TOA data to appropriate distance measurements requires separate modeling of the medium.

A comparative performance study of these three collaborative algorithms in various simulation scenarios is shown in the next chapter.

CHAPTER 4

SIMULATION STUDY

Although theoretical formulation of the three techniques suggests that the synthesized algorithm improves location estimation it does not provide a way to assess the performance of the three collaborative localization algorithms. Hence, the performance of the algorithms is investigated through an extensive simulation study. The impact of several factors in collaborative localization, including effects of sensor node density, reference node density, and deployment strategies of reference nodes are studied in detail through several computer simulations using Matlab.

4.1. Configuration of the Simulation Setup

For the simulation study we assume that N_1 sensor nodes are randomly deployed in a sensor field and N_2 reference nodes are deployed in or around the sensor field. The positions of the reference nodes are assumed to be known apriori and have an absolute error-free position. RSS measurements are collected between two nodes within direct wireless communication range while the coverage of direct wireless communication is determined by the radio transmission range. The radio range is assumed to be isotropic. In this thesis, the log normal shadowing model is used to represent the path loss characteristics of an environment. This assumption is based on analytical evidence presented in [31], [39] and the practical measurement results from [8], [30], [32]. In all simulations, the transmission range is set to -100 dBm and the first-meter received power

is set to -50 dBm, if not explicitly stated otherwise. The standard deviation of the lognormal fading variable is used to introduce an error into the distance estimates for simulation purposes. The true distance is blurred with a zero-mean Gaussian random variable picked from $N(0, \sigma_v^2)$. (The measured distance estimate is equal to the sum of actual distance and an error drawn from the normal distribution $N(0, \sigma_v^2)$). The standard deviation of the lognormal fading variable σ_v set to 6, and the distance-power gradient α set to 3 (α = 2 for ideal free-space channel model), are chosen for all simulations.

Two different sensor network topologies are considered for the simulations: a) uniform random circular field deployment, b) random square field deployment. The first topology is generated using the acceptance-rejection method by generating uniform points in a super-region that encloses the field and rejecting all the points which do not lie within the field. The second topology is obtained by a random generation of the node positions limited by the specified field size. Reference node placement strategies play a key role in improving or reducing the efficiency of a localization algorithm. Reference nodes are placed in two different fashions: a) uniform placement along the border of the field, b) random placement along with the location-unaware sensor nodes. The second case models a deployment such as an air-drop of motes from an unmanned air vehicle (UAV). Both the reference node placement strategies are analyzed and the strategy which maximizes the efficiency of the algorithms is chosen for further analysis. Some of the simulations have been presented in [47].

4.2. Performance of Collaborative Localization Techniques

The performance of MDS is demonstrated using both the sensor network topologies mentioned before. Figure 4.1 shows the result of MDS applied to a sensor field of radius 15 meters with 40 sensor nodes in the uniform-random circular field deployment. In the circular deployment scenario four reference nodes were placed on the border of the field for all the three algorithms. The importance of reference node placement is discussed in the next section. The figure shows the actual locations and the MDS estimated locations connected by a line segment whose length represents the magnitude of estimation error. Figure 4.2 shows the performance of MDS in the random square field deployment. The size of the field is 900 square meters and the number of nodes simulated is 40. In the random square field deployment random reference nodes were generated along with the location-unaware sensor nodes. The root-mean-squared (RMS) location errors of all the sensor nodes for the first and second configurations are 2.8 meters and 3.4 meters respectively. However, these simulations do not imply that MDS performs in a similar way every time. The accuracy varies with the simulation coordinates of the locations of the nodes. It can be observed that MDS has a good convergence property from the above results.

The performance of MLE is observed by applying MLE to the same configurations and scenarios as MDS. The results for the uniform-random circular deployment and random square field deployment are as shown in Figure 4.3. The RMS location errors for both the configurations are 2.2 and 2.4 meters respectively. The RMS location errors of MDS seemed to adhere to a range of values, but behavior of MLE on the other hand

seemed unpredictable. Upon close observation of repetitive simulations with different configurations it was found that MLE was very sensitive to the initial estimate.

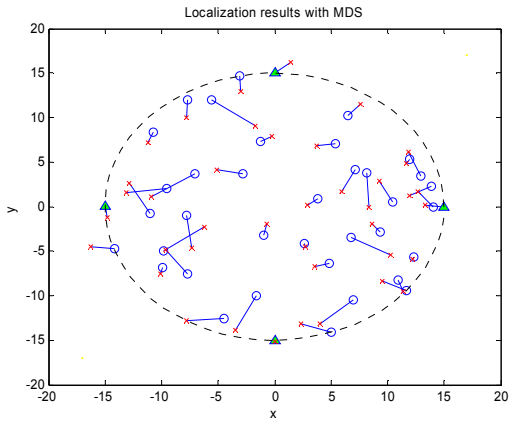

FIGURE 4.1. Localization results with MDS for the uniform-random circular field deployment scenario. o – actual location of sensor node, x – estimation result with MDS, Δ - reference node location, lengths of the line segments between actual and estimated locations represents the magnitude of estimation error for all such simulations.

Though MDS produced fairly good estimates, there was still room for improvement. Since, MLE produced very accurate results in cases where the initial random coordinate matrix was closer to the actual coordinate matrix, it was expected to elevate the accuracy of the MDS estimate. A serial integration of these two methods produced the MDS-MLE algorithm. The rest of this chapter analyzes the performance of MDS-MLE against MDS and MLE.

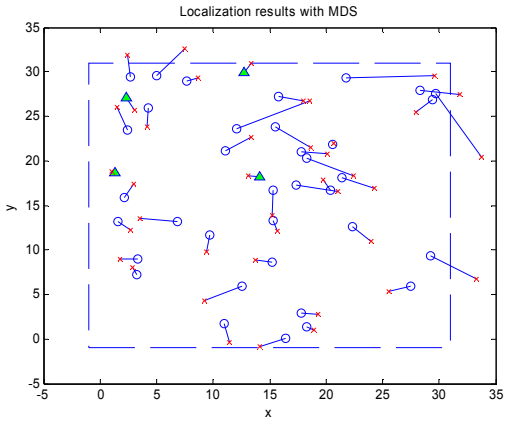

FIGURE 4.2. Localization results with MDS for the random square field deployment scenario. o – actual location of sensor node, x – estimation result with MDS, Δ - reference node location.

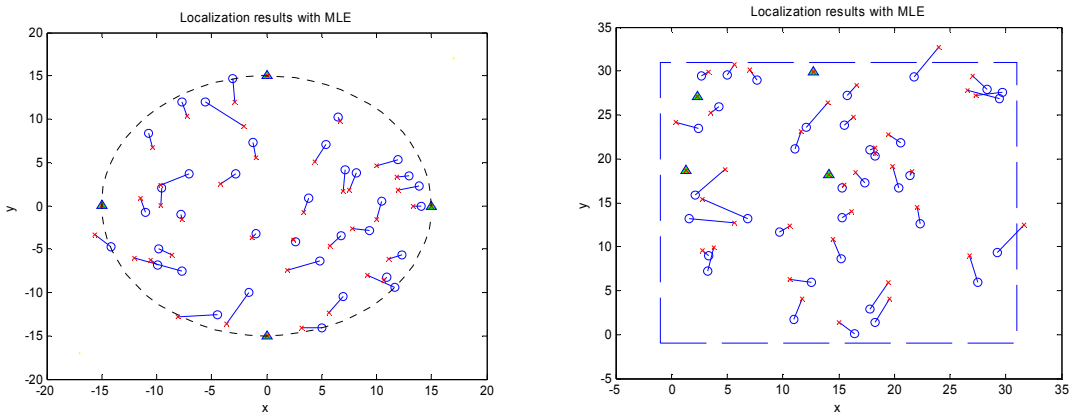

FIGURE 4.3. Localization results with MLE for the uniform-random circular deployment and the random square field deployment scenario. o – actual location of sensor node, x – estimation result with MLE, Δ - reference node location

The efficiency of MDS-MLE is shown through a comparison of the performance of all the three algorithms. The parameters of the simulation remain unchanged (number of nodes = 40, radius of the circular field = 15 meters, size of the square field = 900 square meters, number of reference nodes = 4). A juxtaposition of the MDS and MDS-MLE solutions in Figures 4.2 and 4.4 offer a closer look at how MLE fine-tunes the MDS estimate and improves its accuracy. The RMS location errors of MDS-MLE for the uniform-random circular deployment and for the random square field deployment simulations shown in Figures 4.4 and 4.5 are 2.1m and 2.2m respectively. The improvement in the estimate is evident from the error mitigation. It should be noted that in all the simulations, a random initial estimate of the configuration matrix is first uniformly sampled in the sensor field, and then the same initial estimate is employed in both MDS and MLE (it is understood that MDS-MLE basically uses the same estimate since it only enhances the MDS estimate) to ensure a fair performance comparison of the algorithms.

These simulations are conducted for only a single configuration. In order to study the effect of many parameters on the collaborative localization algorithms such as sensor node density, reference node deployment strategy and reference node density the performance has to be tested at a large-scale, since statistical results from several simulations are often more conclusive in nature.

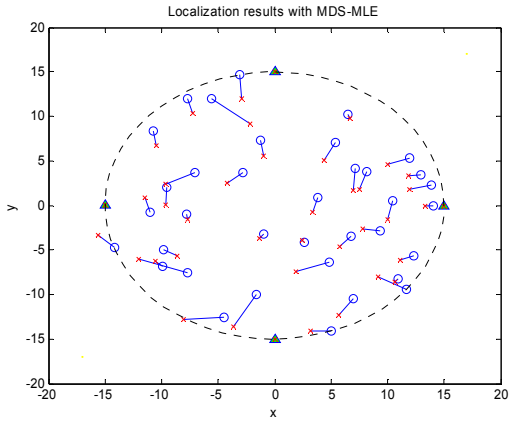

FIGURE 4.4. Localization results of MLE, MDS and MDS-MLE methods on the uniform-random circular deployment scenario. o – actual location of sensor node, x – estimation result with MLE, MDS and MDS-MLE in the respective plots, Δ - reference node location

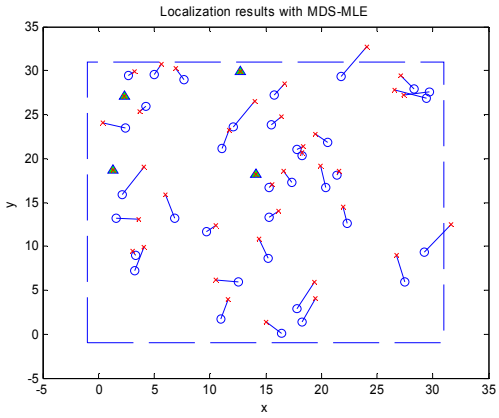

FIGURE 4.5. Localization results of the MDS-MLE method on the random square field deployment scenario. o – actual location of sensor node, x – estimation result with MLE, MDS and MDS-MLE in the respective plots, Δ - reference node location

4.3. Reference Node Deployment Strategies

Reference node positioning strategies play a vital role in improving the accuracy of the location estimates. The deployment geometry of the reference nodes is one of the key factors that significantly influence the performance of localization algorithms. Usually, the reference nodes are either manually placed at optimal locations to cover as many sensor nodes as possible or scattered randomly in the sensor field, such as in the scenario of airborne deployment of sensor networks in hostile or inaccessible environments. An example of the former case is the creation of virtual reference nodes in or around a sensor field by mobile robots. In the latter case, the reference nodes are usually equipped with self-localization devices such as GPS. In this simulation, we compare these two reference node deployment strategies by randomly placing reference nodes within the sensor field in one set of the simulations, and by evenly placing the reference nodes on the border of the sensor field in another set of simulations. The former will be called random reference node placement strategy and the latter border reference node placement strategy. 40 sensor nodes are deployed in a square field of size 900 square meters and a circular field of radius 15 meters.

In the random reference node placement strategy, reference node locations are generated in a fashion similar to the location-unaware sensor nodes. In the border reference node placement strategy, reference nodes are placed at regular intervals on the perimeter of the circle, inscribed in the square-shaped field. Such an arrangement will ensure higher accessibility of the reference nodes to the location-unaware sensor nodes. This does not imply that border reference node placement is the best reference node

positioning strategy. This strategy was used for its ease of implementation and efficiency. Figure 4.6 shows the localization result of the MDS-MLE method on the random scatter of sensor and reference nodes and the result of border placement of reference nodes in a square-shaped sensor field. The RMS location errors of the random reference node placement and the border reference node placement shown in Figure 4.6 are 2.5m and 2.1m respectively.

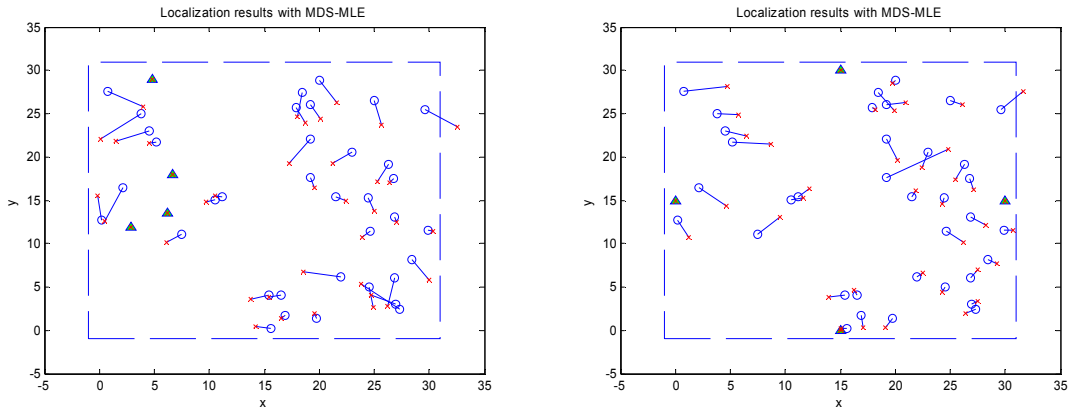

FIGURE 4.6. Random reference node placement and border reference node placement in a random square field deployment. For an unbiased comparison, the same location-unaware sensor node configuration is used in both the cases.

The random placement of reference nodes might sometimes result in the concentration of reference nodes in a small portion of the network. An example of this setting can be seen in the uniform-random circular deployment scenario in Figure 4.8. For the exact same configuration of sensor nodes, the localization results for the border reference node placement scenario appear better than the random reference node

placement scenario. The RMS location errors of the random reference node deployment and the border reference node deployment in the uniform-random circular deployment scenario shown in Figure 4.7 are 4.5m and 1.8m respectively. It can be observed that though such reference node placements could adversely affect the performance of collaborative algorithms, it has limited impact when compared to the performance of traditional localization techniques.

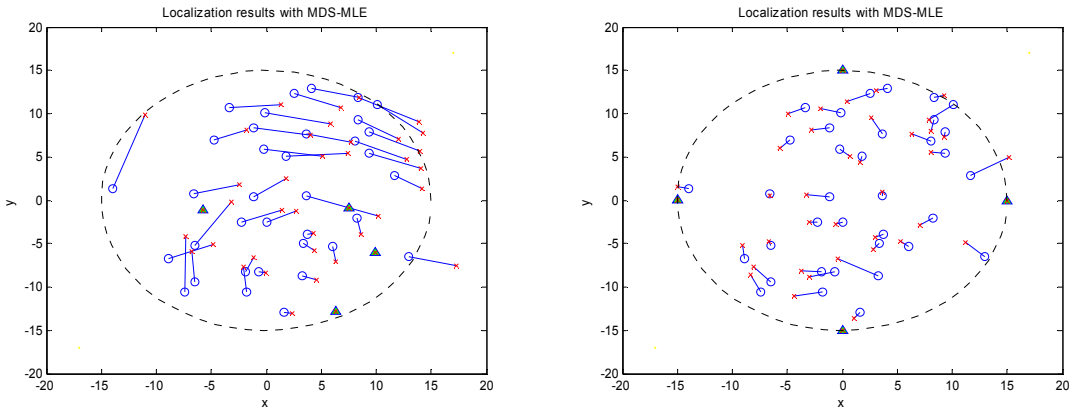

FIGURE 4.7. Random reference node placement and border reference node placement in a uniform-random circular deployment scenario. For an unbiased comparison, the same location-unaware sensor node configuration is used in both the cases.

4.4. Effect of Sensor Node Density

Collaborative localization algorithms use distance estimates collected from location-unaware sensor nodes along with the distance estimates obtained from the reference nodes. The accuracy of a location estimate depends upon the number of distance measurements available from the neighboring nodes. Hence, the density of sensor nodes

in a sensor field plays a major role in the precision of the location estimates. The density of sensor nodes is increased by either increasing the number of sensor nodes within a fixed area or by increasing the sensor field size keeping the number of nodes constant.

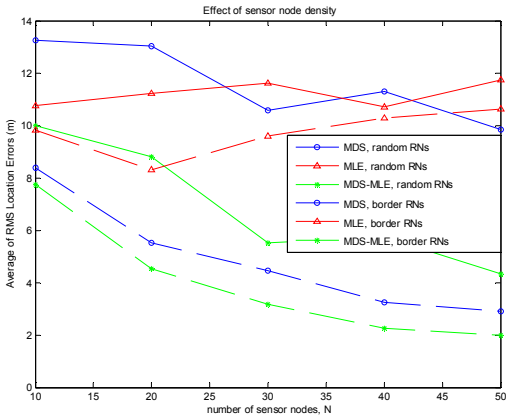

FIGURE 4.8. Average RMS Location Errors of the three algorithms for different densities of sensor nodes in a square field deployment in both the reference node deployment scenarios.

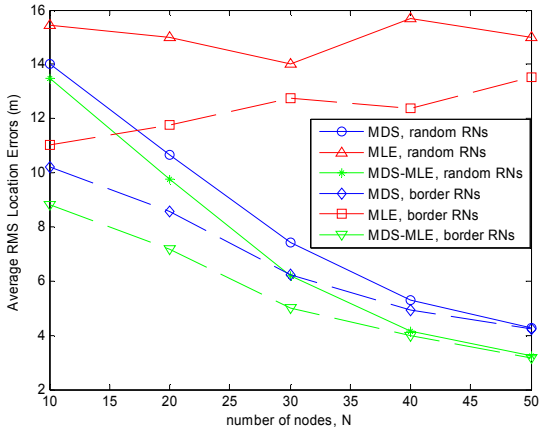

FIGURE 4.9. Average RMS Location Errors of the three algorithms for different densities of sensor nodes in a circular field deployment in both the reference node deployment scenarios.

First, the effect of the density of sensor nodes in a square-shaped sensor field of fixed size is studied. Random sensor nodes are sampled in the field of size 900 sq.m. For each simulation scenario 200 simulations are conducted and the performance of collaborative localization algorithms is compared in terms of average RMS location errors, averaged over 200 simulations. Figure 4.8 shows the average RMS location errors for three different collaborative localization algorithms, i.e., MDS, MLE, and MDS-MLE in the two reference node deployment strategies. The number of nodes, among which five are reference nodes, is increased from 10 to 50 at a step of 10 to study the effects of sensor node density. From the simulation results, it is evident that the average RMS location error decreases steadily as the density of sensor node increases for all algorithms. This is caused due to an increase in the pair-wise distance measurements among the nodes. The same simulation is repeated using a circular field of radius 25 meters. Figure 4.9 shows the result of this simulation. In both circular and square sensor node deployment it can be observed that border reference node deployment produces more accurate results than the random reference node deployment.

Since, border deployment of the reference node produced better statistical results, the rest of the simulations use border deployment strategy of reference nodes. In successive simulations, we only consider the border placement structure of reference nodes in order to concentrate on the study of the effect of other parameters on the performance of collaborative localization algorithms.

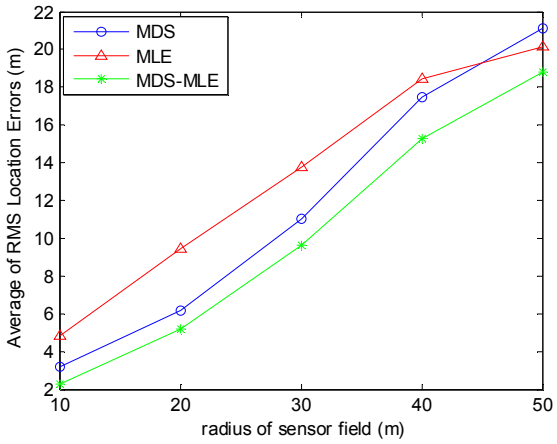

FIGURE 4.10. Average RMS Location Errors for different deployment radius of the circular sensor field.

Next, the effect of density of sensor nodes on the performance of the algorithms is illustrated by varying the size of the sensor field while keeping the number of sensor nodes constant at 30. The effect is studied in the circular and the square sensor field by varying the radius and the side of the sensor field from 10 m to 50 m respectively. Four reference nodes are deployed uniformly on the border of the sensor field. From the simulation results presented in Figures 4.10 and 4.11, it is clear that MDS-MLE performs better than the other two algorithms consistently. For example, the average RMS location errors of MLE, MDS and MDS-MLE for the circular sensor field of radius 10 m are 4.80 m, 3.16 m, 2.24 m respectively and for a radius of 40 m, they are 18.46 m, 17.47 m and 15.30 m respectively. It is also seen that the average RMS location errors increase as the size of the sensor field increases, that is, as the density of the sensor node decreases. This is because, as the sensor network becomes sparse, less and less RSS will

be measurable among the nodes due to the fixed radio range of the nodes. The performance deteriorates in cases where the sensor nodes are spread out so far that they are out of the communication range of many other nodes. As a summary, the MDS-MLE algorithm appears to perform better than MDS and MLE, though all three algorithms exhibit a similar behavior as the size of sensor field varies.

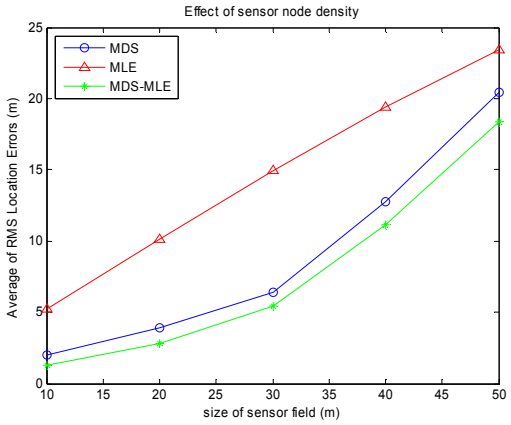

FIGURE 4.11. Average RMS Location Errors for different deployment size of the square-shaped sensor field.

4.5. Effect of the Density of Reference Nodes

The number of reference nodes employed in collaborative localization greatly affects the estimation performance of unknown sensor node locations. The next simulation is designed to study this effect, where the number of reference nodes is varied while keeping all the other parameters constant. The simulation is started with 3 reference nodes and increased up to 10 reference nodes. The radius of the circular sensor field is 30 m and the size of the square field is 900 sq.m. The number of nodes is kept constant at 40. Figure 4.12 shows the effect of density of the reference nodes in a random square

field deployment scenario along with the performance of MDS, MLE and MDS-MLE algorithms in all the configurations. For all the successive simulations, the average RMS location errors are calculated since the performance of an algorithm cannot be assessed from a single configuration.

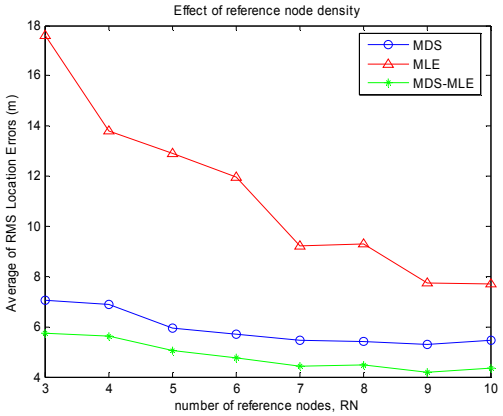

FIGURE 4.12. Average RMS location error for different reference node densities in a random square field deployment.

Figure 4.13 shows the variation of the performance of the three collaborative localization algorithms in a uniform-random circular deployment scenario with a change in the density of reference nodes. From the results, it can be observed that the performance of all three algorithms improves as the number of reference nodes increase. The average RMS location error of MLE reduces drastically from 17.59 m to 7.723 m and 16.72m to 7.17m in Figures 4.9 and 4.10 respectively as the number of reference nodes increase from 3 to 10. The effect of the reference node density was more pronounced in MLE than MDS and MDS-MLE, as seen from the little variation in the average RMS location error two algorithms. Though the average RMS location error of

MDS is consistently low, MDS-MLE out-performs MDS throughout all the simulation scenarios.

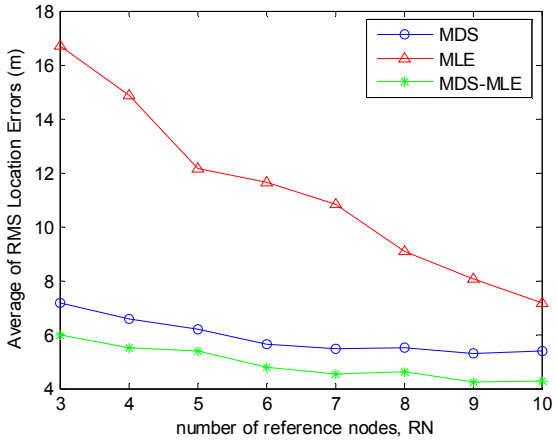

FIGURE 4.13. Average RMS location error for different reference node densities in a uniform-random circular field deployment.

4.6. Effect of Distance Estimation Errors

The distance estimates collected from a real-time sensor network are not very accurate. In order to model the implicit errors in distance estimates, the actual distance estimates are blurred with a Gaussian noise with a standard deviation σ_v for simulation purposes. In this simulation the performance of the three algorithms is studied through a variation of the standard deviation of the log-normal shadowing model in distance estimates. For the simulation, we use a square sensor field of size 900 sq.m. with 40 sensor nodes and 4 reference nodes. The standard deviation parameter σ_v, which characterizes the noise in a channel is varied from 3 to 7. All the preceding simulations assumed a standard deviation of 6. Figure 4.14 shows that the performance of the three

algorithms declines slowly with an increase in the noise of the distance measurements. However, it can be observed that the average RMS location errors are still in an acceptable range. The performance of the MDS-MLE algorithm is optimum when the distance estimates are error-free.

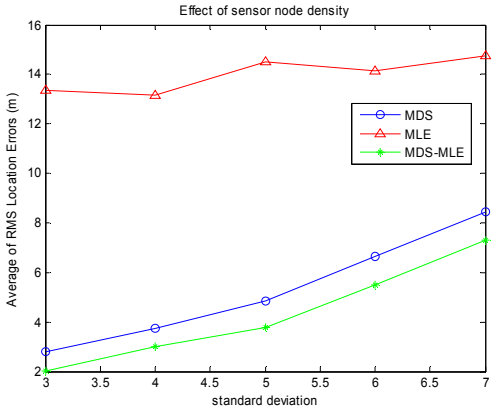

FIGURE 4.14. Average RMS Location Errors for different values of the standard deviation of the log-normal shadowing model in a square-field deployment.

4.7. Summary

From the various simulation results, it can be concluded that all the three collaborative localization algorithms tend to perform better when the sensor field is densely deployed. The algorithms also show a better performance when reference nodes are deployed uniformly on the border of a sensor field than when they are randomly deployed inside the sensor field along with the location-unaware sensor nodes. The comparative study results presented in this chapter provide a greater insight into the factors affecting the performance of collaborative localization algorithms.

CHAPTER 5

DEVELOPMENT OF WIRELESS SENSOR NETWORK TESTBED

The previous chapter discussed the performance of the localization algorithms in simulation conditions. Though simulation is a powerful tool, real-time deployment uncovers several issues in radio signal propagation which are not discovered otherwise. Hence, the performance of the algorithms is tested in an experimental setup which will investigate the feasibility of using RSS-based distance measures. This chapter describes the hardware used in the experimental setup and the software used to program the wireless sensor nodes. The requirements of the program used for data collection are discussed in section 5.3 along with the format of the messages exchanged between nodes.

5.1. Hardware

The experiments for RSS-based location estimation were conducted on Crossbow's MPR400 Mica2 motes with 916MHz multi-channel radio transceiver [40]. The MPR400 has Atmel Atmega128L, a low power microcontroller which runs TinyOS from its internal flash memory. Mica2 motes have a Chipcon CC1000 radio, which uses FSK modulation [41] and has a built-in Received Signal Strength Indicator (RSSI) sampled by a 10-bit ADC. Figure 5.1 shows MTS310CA, a sensor board which can be attached to the radio platform via the 51-pin connector. MTS310CA has sensors to detect light, temperature, sound, magnetic fields and vibrations. In this thesis, the sensor board is not required for location sensing. Mica2 motes run on 2 AA batteries and are programmed

using Crossbow's programming and serial interface board MIB510CA. In addition to the RS-232 serial programming interface, the MIB510CA allows for sensor network data aggregation on a PC as well as other standard computer platforms [42]. Any Mica2 mote can operate as the base station when plugged into the serial interface board through the 51 pin connector.

FIGURE 5.1. Mica2 Mote

FIGURE 5.2. MIB510 programming board

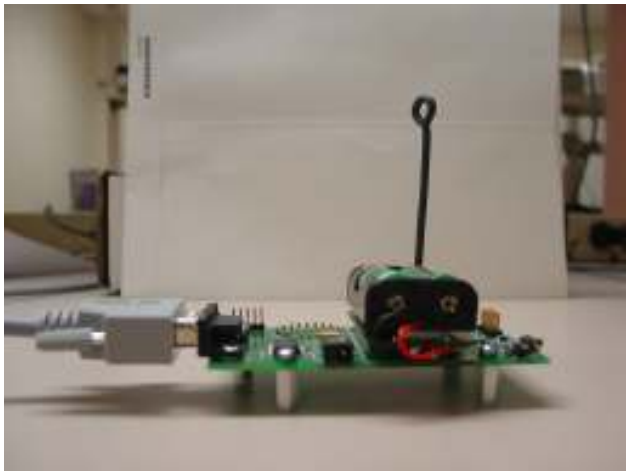

FIGURE 5.3. MIB510CA with the Mica2 mote attached

5.2. Software

The Mica2 motes are programmed in nesC, a component-oriented language for networked embedded applications. nesC is used as the programming language for TinyOS, an open-source operating system designed for wireless sensor networks with severe power and memory constraints. nesC is being widely used by several wireless sensor networks research groups because it incorporates TinyOS's event-driven concurrent execution and a component-oriented application design [43]. NesC has a C-like syntax, but supports the TinyOS concurrency model, as well as mechanisms for structuring, naming, and linking together software components into robust network embedded systems [44]. The chief aim is to allow programmers to build applications out of components with well-defined, bi-directional interfaces.

Due to its flexibility and ease of implementation, nesC was used to program the mica2 sensor nodes. The program uses multi-hop communication to direct the

measurements acquired by a sensor node to the central base station where location estimation is performed. Multi-hop based applications are capable of collecting data from nodes not in the range of the base station. The TinyOS-1.1 release and later include library components that provide ad-hoc multi-hop routing. A collection-tree based algorithm, rooted at the base station is designed for the experiment in order to log the measurements made by all the sensor nodes at the base station.

The features of the program used for RSS data collection from the sensor network are as follows:

1. Each node is programmed to broadcast a message announcing its presence once every fixed time interval. The message contains the node ID of the broadcaster (See Figure 5.4). The MAC layer of TinyOS takes care of the channel access negotiation and channel contention problems. (The sensor nodes can be sequenced by the node ID numbers, if ordered broadcasts are desired. Another alternative is to use a random number generation function to decide the schedule of a broadcast.) For clarity purposes, this message shall be referred to as Message1 in the rest of the chapter.
2. Each node listens to the neighbors broadcast and records the received signal strength of the message. These readings are encapsulated in a message (See Figure 5.5) and sent to the base station. The message sent to the base station contains four fields: a) source ID or node ID of the transmitter / broadcaster, b) RSS value of the message received from the source node, c) destination ID or node ID of the receiver d) battery value of the receiver or destination node.

For clarity purposes, this message shall be referred to as Message2 in the rest of the chapter.

This program can be optimized by reducing the energy expended in communication by a store and forward method. The sensor nodes can be programmed to store the readings in the flash memory and then send them to the base station when the memory is full. Further, the size of the packet can be reduced by computing the mean of duplicate readings. Multiple readings between node pairs can help to reduce errors in distance estimates caused by constructive or destructive interference. For the localization experiment each node broadcasts multiple messages within a time interval, resulting in several pair-wise measurements per node-pair.

Message Header	Source node ID	battery voltage value of the source node

FIGURE 5.4. Format of the Message1 broadcasted by each sensor node periodically in the network.

Message Header	Source node ID	RSS value of the message as received at the destination from the source	Destination node ID	battery voltage value of the destination node

FIGURE 5.5. Format of the Message2 sent to the base station. Each sensor node sends a message of this type to the base station as soon as it listens to a broadcast of its neighboring node

The broadcast messages or messages of type Message1 are only intended for the neighbors of a sensor node (nodes within its range) whereas the data logging messages or messages of type Message2 are sent to the base station using multi-hop if necessary. TinyOS includes library components that provide ad-hoc multi hop routing to sensor network applications. It is implemented using a shortest-path-first algorithm with a single destination. The multi-hop implementation consists of two core modules, MultiHopEngineM and MultiHopLEPSM, wired together in the MultiHopRouter configuration [44]. For the localization experiment, a component called RSSI was developed using the default components. TinyOS frees the user from the hassle of developing lower level communication and routing layers. The LedsC component which provides an interface to use the leds on the Mica2 board is used for visual confirmation of events like a successful Send() or Receive(). The leds have proven to be very useful during debugging. The TimerC component is used to trigger the broadcasts of Message1. The Comm component takes care of communication of the broadcast messages.

5.3. Conversion of ADC value to RSSI

The CC1000 radio chip present on the Mica2 board has a built-in received signal strength indicator (RSSI) giving an analogue output signal at the RSSI/IF pin [41]. The output current of this pin is inversely proportional to the input signal level. It is obtained at the ADC channel 0 of the radio board and is recorded by default as strength in the TOS_Msg structure of TinyOS. The value of the RSSI of a message depends on the battery voltage of the receiver. (5.1) is used to obtain the RSSI voltage value from the

raw ADC value. The equations used to convert the ADC Counts to RSSI in dBm for the 916MHz motes are [46],

(5.1) $$V_{RSSI} = V_{batt} * ADC\_Counts / 1024 ,$$

(5.2) $$RSSI(dBm) = -50.0 * V_{RSSI} - 45.5 ,$$

where V_{batt} is the battery voltage of the receiver node, and ADC_Counts is the data obtained from the ADC measurement of channel 0. The Mica2 battery voltage, V_{batt} can be obtained by the following [34]:

1. Set the BAT_MON processor pin (PA5/AD5) to HI.
2. Program the application code to measure ADC Channel 7.
3. Compute battery voltage, V_{batt}, from Channel 7's data as,

(5.3) $$V_{batt} = V_{ref} * ADC\_FS / ADC\_Count ,$$

where V_{batt} is the battery voltage, ADC_FS is the ADC full-scale voltage span and is equal to 1024 and V_{ref} is the external voltage reference equal to 1.223V for a mica2 and ADC_Count is the data from the ADC measurement of channel 7. Both, the RSS value and the battery voltage values are recorded in 2 bytes.

5.4. Data Collection

The RSS data from the sensor network is collected by a computer connected to the programming board used as the base station. One of the motes is plugged onto the programming board so that it can sense the network data and forward it to the computer. Before deployment when the motes are installed with the program, the node ID of the

mote connected to the base station is set as 0 since our root-based multi-hop application designates the mote with node ID zero as the base station. Post-deployment, raw data arriving at the base station is logged into flat files using a java program.

Messages received on the base station are in a reverse-ordered hexadecimal format. The necessary fields are shelled out from each packet and converted to decimal system. The RSS values are computed using (5.1), (5.2) and (5.3) and stored in flat files. These values are converted to distance estimates using a known path loss model (environment-specific path loss modeling will be discussed in the next chapter). An $N \times N$ distance matrix is formed by calculating the pair-wise distance estimates for a sensor network of N nodes. These distance matrices are supplied to the localization algorithm for location estimation. If every node can listen to all the other nodes in the network, a total of $N \times (N-1)$ readings will be recorded.

These distance matrices will be used as the input to the localization system implemented using Matlab. The localization system produces a plot of the estimated locations which can be mapped onto the field layout diagram if need be.

CHAPTER 6

EXPERIMENTAL STUDY OF RSS-BASED LOCALIZATION TECHNIQUES

In this chapter, practical issues associated with distance estimation using received signal strength measurements which affect the accuracy of any RSS-based localization solution are described. Multipath fading effects introduce substantial error in RSS-based distance estimates. Area–specific path loss models obtained through environmental modeling in wireless sensor networks subdue the effects of shadow. Environment-dependent parameters such as first-meter power loss and distance power gradient determined from the lognormal shadowing model are utilized to convert the RSSI power measurements to the respective distance measurements. Performance of all the three collaborative localization algorithms is evaluated through a localization experiment and simulations based on parameters obtained through modeling.

6.1. Variability of Received Signal Strength

Several localization systems use received signal strength to estimate distance between transmitter and receiver. Received signal strength is often regarded as an unreliable indicator of distance indoors due to absorption and reflection of the radio waves by obstacles. Apart from multipath fading and shadowing, received signal strength is also affected by variation across radios. There is a high variability among sensor nodes due to mass-production of the hardware. In order to characterize the discrepancies in the motes, experiments were conducted in an indoor environment with no furniture or other

obstacles. All the experiments in this section were conducted in the lobby near the south wing entrance of the College of Engineering at UNT, unless specified otherwise.

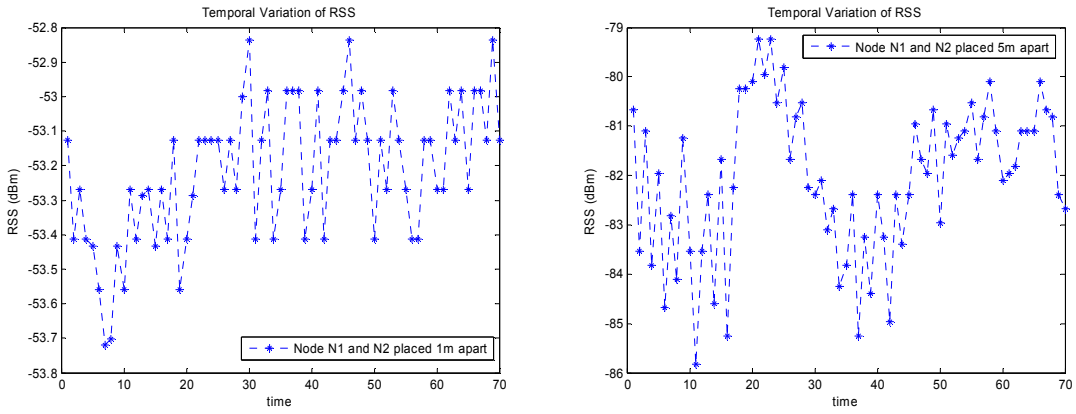

FIGURE 6.1. Temporal Variability of RSS. Two samples of received signal strength measurements are collected over time from a randomly selected transmitter-receiver pair (N_1 & N_2). For the first sample, the pair was placed 1 meter apart and for the second, the pair was placed 5 meters apart.

The received signal strength of messages received by a node from a specific transmitter varies over time due to several factors such as background interference or multipath fading and shadowing. The temporal variability in RSS from a stationary transmitter-receiver pair can be seen in Figure 6.1. RSS measurements were collected by placing the pair 1 meter apart. Measurements are repeated using the same pair and increasing the separation distance to 5 meters. The conditions of the environment are kept constant throughout the experiment. It can be observed that the same node pair does not produce a constant RSS value over time. The standard deviation about the mean of the

readings when the separation distance is 1 meter is 0.21 dBm compared to 1.67 dBm when the separation distance is 5 meters. The fluctuations due to fading effects are negligible at a distance of 1 meter due to direct line of sight conditions and absence of obstacles within such a short distance. The effects of multipath fading are more significant when the separation distance is 5 meters. The temporal variability of RSS due to fading can be reduced through path loss modeling which will be discussed in the following section.

In our experiments, the transmit power of the radio is highly dependent on the battery of the mote. The received signal strength measurement is dependent on the transmit power of a mote. Different battery levels in a sensor network can cause transmitter variability which is illustrated in the Figure 6.2. In this experiment, multiple transmitters are configured to transmit to a single receiver and the received signal strength measurements are recorded at the receiver. In order to ensure a fair comparison, the experiment is repeated for each transmitter in identical environmental settings. The absolute positions and orientations of the transmitters and the receiver do not change in any of the experimental runs. Figure 6.2 shows the RSS measurements collected by a receiver from two different transmitters at two battery levels: full and low. Node N_1 is used as the receiver and nodes N_2 and N_3 are used as transmitters. Transmitter variability is reduced by installing fresh batteries in all the motes in the beginning of the experiment.

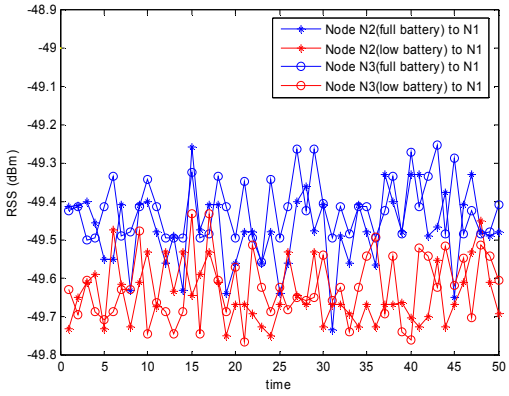

FIGURE 6.2. Transmitter Variability. Received signal strength measurements are collected at a single receiver N_1, when two transmitters N_2 and N_3 transmit from the same position, 1 meter away from the receiver, at different time instants.

Receiver variability can be characterized in a similar fashion by using two receivers and a single transmitter. Figure 6.3 shows the variability of two receivers when placed in the same position, separated temporally. The transmitter-receiver pairs were placed 1 meter apart. The standard deviation of RSS measurements due to receiver variability is very negligible when compared to the value of standard deviation of RSS measurements due to fading effects (generally in the order of 6-10 dBm). Path loss modeling is used in this thesis to reduce the effects of multipath fading.

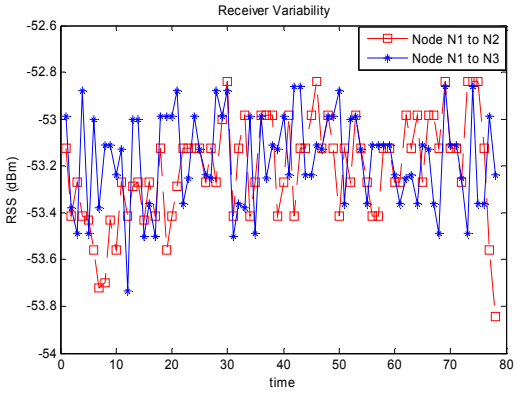

FIGURE 6.3. Receiver Variability. The received signal strength collected at two receivers N_2 and N_3, each placed 1 meter away at the same position and orientation from transmitter N_1, at different time instants.

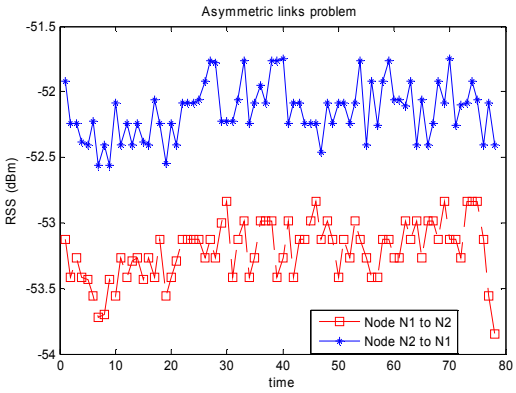

FIGURE 6.4. An illustration of the asymmetric links problem. Though, the two sets of readings were collected simultaneously under similar conditions, the variation between the two RSS values depicts the asymmetry in communication links.

Link asymmetry can be observed usually when two nodes mutually exchanging

messages transmit at different power levels. Variations due to asymmetry of communication links is depicted in Figure 6.4. RSS measurements of the messages transmitted between Nodes N_1 and N_2 separated by a distance of 1 meter were recorded.

6.2. Radio Propagation Path Loss Modeling

In this thesis, the lognormal shadowing model is used to represent the path loss characteristics of an environment. The distance can be related to RSS through the classic pathloss model [29],

(6.1) $$L_p = L_0 10\alpha \log_{10} d + v \ ,$$

where L_0 is the signal power loss in dB unit at 1 m distance, L_{p} is signal power loss in dB at a distance d ($d \geq 1\mathrm{m}$), the parameter α is distance-power gradient (also known as pathloss exponent), and v is a Gaussian random variable representing log-normal shadow fading effects in complex multipath environments. In the literature of radio propagation channel studies, the random variable v is considered zero-mean, that is, $v \sim N(0, \sigma_v^2)$, while the value of the standard deviation σ_v depends on the characteristics of a specific multipath environment. Equivalently, (6.1) can be written as

(6.2) $$P_{ij} = P_0 - 10\alpha \log_{10} d_{ij} - v_{ij} \ ,$$

for $1 \leq i \leq N$ and, $1 \leq j \leq N$ where P_0 is the received power in dBm unit at a distance of $1\mathrm{m}$, d_{ij} is the distance between node i and node j, p_{ij} is the received power in dBm measured at node j (transmitted by node i) and v is a Gaussian random variable representing log-normal shadow fading effects in complex multipath environments. In

the literature of radio propagation channel studies, the random variable v is considered zero-mean, that is, $v \sim N(0, \sigma_v^2)$, while the value of the standard deviation σ_v depends on the characteristics of a specific multipath environment. Distance between a pair of nodes can be calculated using,

$$d_{ij} = 10^{(P_0 - P_{ij})/(10\alpha)}, \tag{6.3}$$

provided the first-meter received power P_0 and the path loss exponent α are given. Linear regression is used to determine these unknown parameters. Since RSS measurements made at 1 meter distance are considered accurate [29], the reference distance is chosen as 1 meter.

To determine the path loss exponent or the distance power gradient of a given radio propagation channel, an extensive measurement campaign was undertaken in the lobby near the South Wing entrance of the College of Engineering at UNT. Three nodes N1, N2 and N3 were picked randomly for modeling. The antenna height of all the nodes is 4 inches by default. Node N1 served as the base station and collected measurements from N2 and N3 one at a time. RSS measurements were collected at known distances of 1, 2, 3, 5, 8 and 10 meters. 50 readings are recorded over time for each distance by both the node pairs. The scatter plot resulting from these measurements can be seen in Figure 6.5. The received signal strength at a distance of 1 meter has very little variation and is chosen as the reference measurement. Hence, P_0 is fixed at the mean value of the received signal power at 1 meter distance. The path loss exponent of a model is obtained by applying linear regression to the RSS measurement data. The best-fit line obtained from regression

passes through P_0 as seen in Figure 6.5. In this experiment, the values of distance power gradient, first-meter received signal strength and standard deviation are obtained as 2.64, -52.38 dBm and 5.12dBm respectively.

TABLE 6.1. Path loss modeling parameters of various environments

Environment	P_0 (dBm)	α	σ_v (dBm)
Indoor - no obstacles	-52.38	2.64	1.05
Indoor - with doubled antenna height	-50.51	1.69	2.29
Indoor Corridor	-52.73	1.98	3.70
Outdoor	-54.51	4.44	1.32

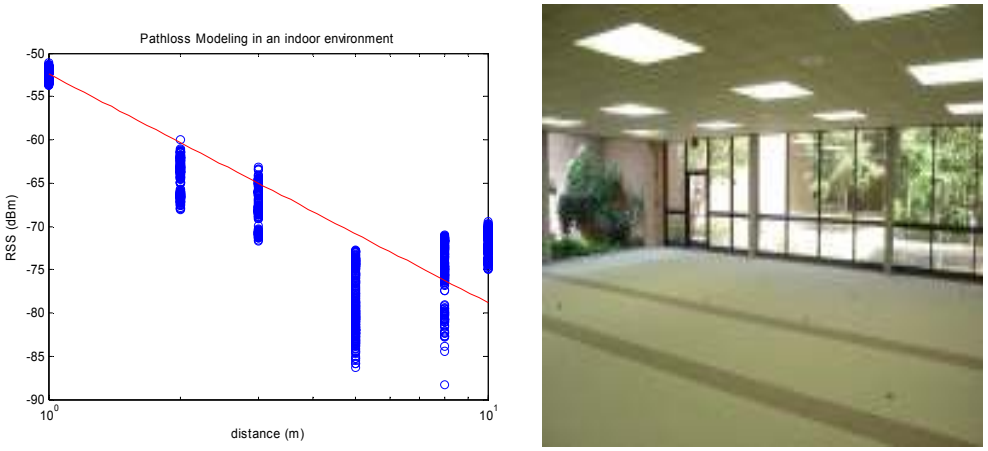

FIGURE 6.5. Modeling an indoor environment using measurements collected from the lobby near the South Wing entrance of the College of Engineering at UNT. The environment-specific parameters are determined using linear regression.

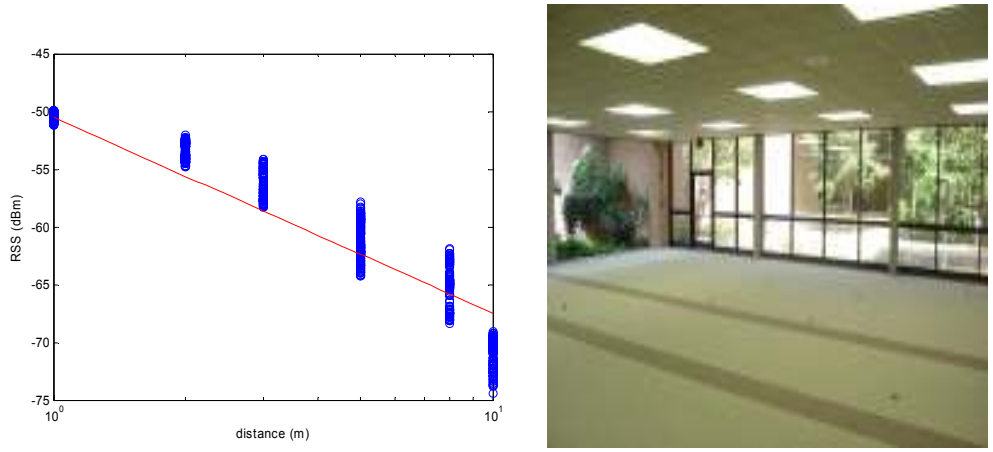

FIGURE 6.6. Modeling the same indoor environment as Figure 6.6, except the height of the antennas is increased by 4.4 inches.

The same experiment is repeated by increasing the height of antennas of all the nodes by 4.4 inches. The path loss model in this case is obtained as shown in Figure 6.6. From the path loss model, the distance power gradient is obtained as 1.695, the first-meter power loss is obtained as -50.5 dBm and the value of standard deviation is obtained as 2.29. The path loss exponent differs from environment to environment. However, a pre-deployment area-specific training phase will ensure that the path loss exponent of an environment is estimated before-hand. To illustrate the variability of path loss characteristics of an environment, the modeling was conducted in two more environments: a corridor (the main corridor in the Department of Electrical Engineering, Research Park, UNT. See Figure 6.7) and an open outdoor space (parking lot near the North East wing of the Research Park at UNT, see Figure 6.8). The advantage of collecting these models is that they can be used to develop a simulation environment for future research purposes. Figures 6.7 and 6.8 show the path loss models of the indoor

corridor and outdoor environments respectively. Table 6.1 displays the values of the environment-dependent parameters for the four experimental scenarios.

Using the linear regression line, the discrepancy between the actual and the expected distance measurements can be computed as,

$$e = P_{observed} - P_0 - 10\,\alpha \log_{10} d_{original}\,, \tag{6.4}$$

where $P_{observed}$ is the received signal power obtained at distance $d_{original}$ and α is the distance-power gradient obtained from the path loss model. Figure 6.9 shows the normal plot of the distance measurement error data. The mean of the error data is obtained as -1.05 dBm and the standard deviation of the normal data is obtained as 5.12 dBm. The lower and upper bounds of the mean at 95% confidence intervals are -1.30 dBm and -0.8 dBm respectively. The linearity of the error data indicates that the sample can be modeled by a normal distribution. Kolmogorov-Smirnov normality test was conducted to check the normality of the error data and only the residuals in the outdoor scenario passed the test at 0.03 significance level. Since, the experiments were conducted only for a single sample of data, it cannot be said that the residuals do not model log-normal distribution. Several ranging experiments will be conducted in the future to draw further conclusions.

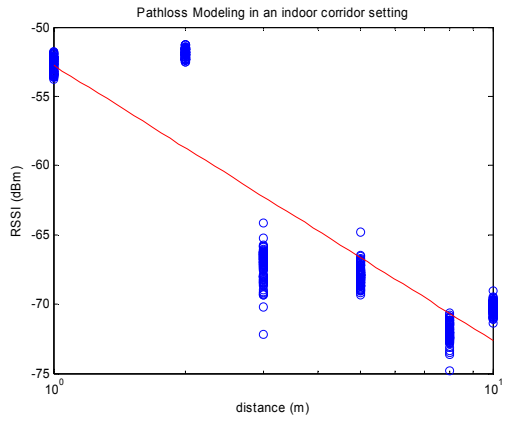

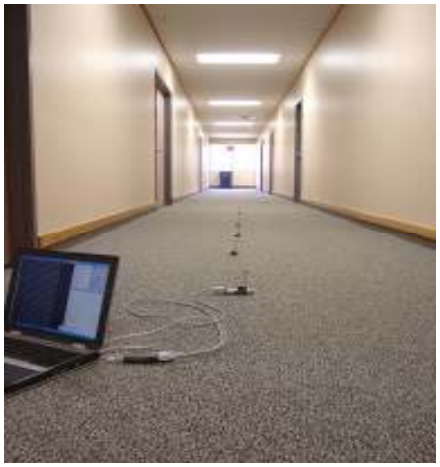

FIGURE 6.7. Measurement of environment-dependent parameters in the indoor corridor shown.

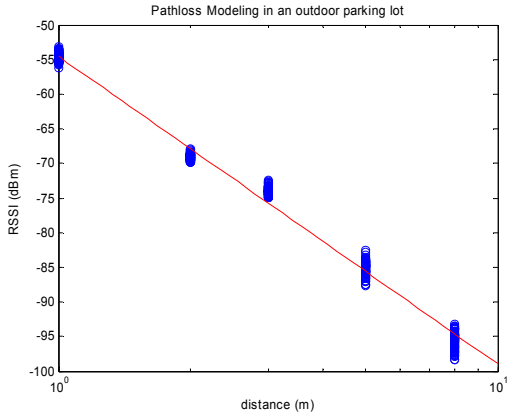

FIGURE 6.8. Measurement of environment-dependent parameters in the outdoor parking lot shown.

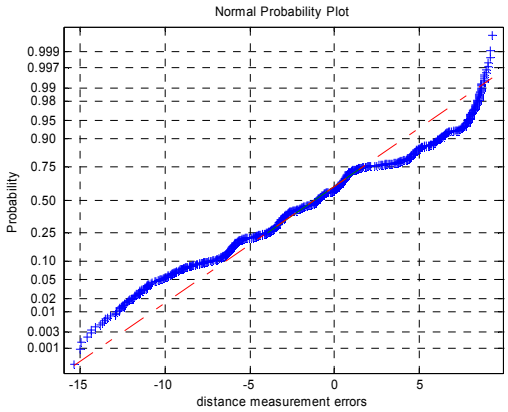

FIGURE 6.9. Normal distribution plot for normality testing of the distance measurement errors of the indoor setup modeled in Figure 6.5.

6.3. Localization Experiment

Once the path loss modeling of an environment was completed, the proposed localization algorithm was tested on an experimental setup. The experiment was conducted in the lobby near the south wing entrance of the College of Engineering at UNT. Eight Mica2 nodes were placed as shown in Figure 6.10, covering an area of 81 square meters. Four reference nodes (RNs) forming the outer square were placed in the corners of a square of side 9 meters and the four location-unaware sensor nodes (SNs) to be localized were placed in the corners of an inner square of side 3 meters as shown in Figure 6.11. Each SN is horizontally and vertically 3 meters away from the nearest RN. The four location-unaware sensor nodes were introduced one at a time into the network to observe for improvements in location estimation with an increase in the number of sensor node measurements. Border deployment strategy of reference nodes is chosen due to its favorable performance in the simulation scenarios. A very basic setup was chosen for the

experiment due to lack of similar hardware. The experiment will be extended to a larger sensor network in the future. The hardware and software used for the experiments was discussed in Chapter 5.

FIGURE 6.10. Experimental setup in the lobby near the south wing entrance of the College of Engineering at UNT. The circles in the indoor environment depict location-unaware sensor nodes and the boxes show the reference nodes deployed on the border.

All the sensor nodes including the reference nodes transmit broadcast messages periodically and record the RSS value of the messages they receive. Readings are logged for a fixed time period after which the network goes to sleep for a specific amount of

time. The data collection procedure was repeated over a period of time until hundred such data sets were recorded. Multiple data sets were collected in order to demonstrate the performance of the algorithms statistically. In each data set, multiple RSS measurements were obtained per node pair. All the RSS measurements were aggregated pair-wise and averaged in order to reduce the effect of propagation errors. The distance power gradient and first-meter power loss obtained in path loss modeling of the indoor environment (shown in Figure 6.5) are employed to convert the signal loss to distance estimates in the localization experiment.

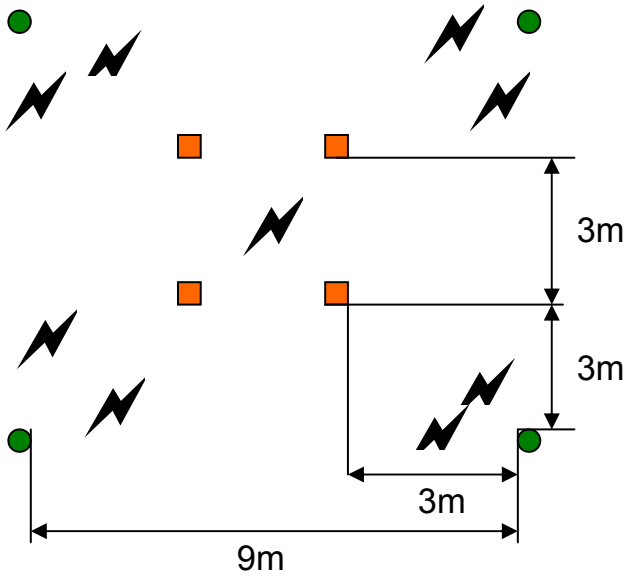

FIGURE 6.11. Layout of the experimental deployment. The green circles on the border represent reference nodes and the orange squares represent location-unaware sensor nodes. Each node collects RSS measurements from all the other nodes in the network.

Figure 6.12 shows the statistical result of localization of sensor nodes over hundred

data sets. MDS seems to perform better than the other algorithms in contrast to the simulation results. The average root mean square (RMS) location errors of MDS, MLE and MDS-MLE solutions are 2.9 meters, 8 meters and 5 meters respectively. The effect of density of the nodes cannot be determined exactly from the shape of the graph. However, when the number of sensor nodes is 4, the performance of MDS and MDS-MLE seem to converge.

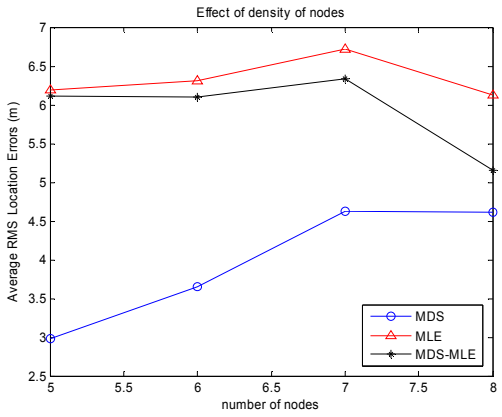

FIGURE 6.12. Localization results from the experiment conducted in the indoor lobby.

Performance of an algorithm cannot be assessed through just a single scenario. The same experiment was recreated in simulation conditions employing similar sensor location configuration and environment-dependent parameters used in the experiment. A standard deviation of 5.12 dBm derived from the path loss modeling of the indoor environment was introduced to bias the distance measurements in the simulations. The simulations were repeated for two hundred times in order to obtain statistically conclusive results. Figure 6.13 shows the result of these simulations. The average root

mean square (RMS) location errors of MDS, MLE and MDS-MLE solutions are 3.2 meters, 2.7 meters and 2.9 meters respectively. The performance of MLE reflects the fact that it tends to perform well for a small sample size.

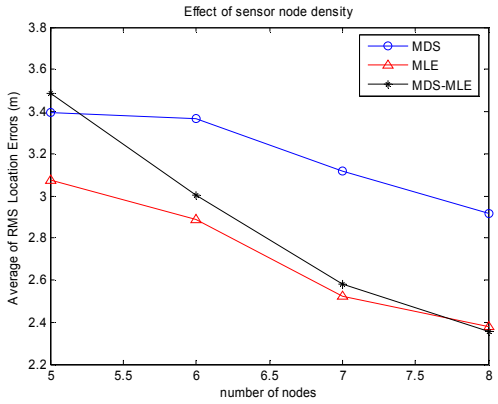

FIGURE 6.13. Localization results from the simulations conducted using the exact same configurations and parameters as the experiment conducted in the indoor lobby.

The advantage of modeling different sensor fields is that the performance analysis of different algorithms can be done through simulations using an arbitrary number of sensor nodes in an arbitrary field size. Since the experimental setup was limited by the number of sensor nodes, it could not provide an accurate view of the performance of the collaborative localization algorithms. Hence, the experiment was simulated again, by increasing the number of sensor nodes to 25 this time in a 625 sq.m. sensor field. The environment-specific parameters derived from the indoor lobby experiment were used for the simulation. The sensor nodes were placed in a 5×5 grid and a standard deviation of 5.12 dBm was used to bias the distance estimates. The reference nodes were placed as

shown in Figure 6.14 on the border of the field. The average root mean square (RMS) location errors of MDS, MLE and MDS-MLE solutions were obtained 3.4 meters, 4.3 meters and 2.9 meters respectively. Simulations such as these allow the study of different factors on the three algorithms with statistical results.

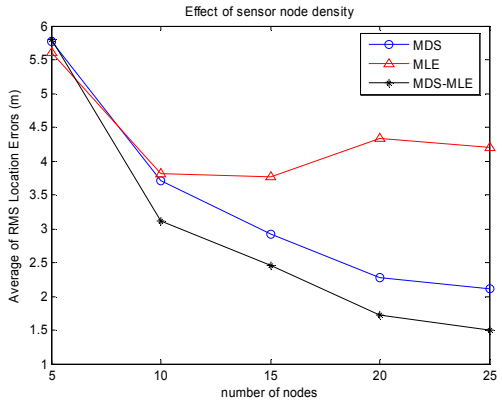

FIGURE 6.14. Localization results from the simulations conducted using environment-specific parameters derived from the experiment conducted in the indoor lobby.

6.4. Summary

In this chapter, the different factors responsible for variation of received signal strength measurements were presented. Path loss models of different environments were studied to depict the variation of environment-specific parameters. The parameters produced by these models are later on used for statistical simulation studies. The three collaborative localization algorithms were studied in experimental settings. The result was inconclusive because the experiment was conducted in the same setting without much difference in the environment. However, the simulation study using experimental

parameters was useful to draw several statistical conclusions. A comparison of the results of the three collaborative techniques studied in this thesis with the results of other localization techniques is not easy since performance testing results in the same environmental conditions are not available.

CHAPTER 7

FUTURE WORK

The current localization system collects RSS measurements from the sensor network using a java program and performs localization on the data through Matlab code. We intend to enhance the application by making the localization system work in real-time, such that the data gathered from the network is forwarded via one of the reference nodes to the computer. The localization system computes the locations of all the nodes on-the-fly using the knowledge of the location of all the reference nodes. The resultant sensor node locations can be graphically mapped onto the layout of a building or a sensor field. The map can be updated periodically by collecting ranging data at regular intervals and performing localization of the nodes. This will allow the user to observe a change in the location of a sensor node or the effect of external factors such as human motion in the sensor field.

BIBLIOGRAPHY

[1] I.F. Akyildiz, W. Su, Y. Sankarasubramaniam, and E. Cayirci, "A survey on sensor networks", *IEEE Communications Magazine*, vol. 40, no. 2, pp. 102-114, Aug. 2002.

[2] G.J. Pottie and W.J. Kaiser, "Wireless integrated network sensors", *Communications of the ACM*, vol. 43, no. 5, pp. 51-58, May 2000.

[3] C.-Y. Chong, and S.P. Kumar, "Sensor networks: Evolution, opportunities, and challenges", *Proceedings of the IEEE*, vol. 91, no. 8, pp. 1247-1256, Aug. 2003.

[4] J.M. Rabaey, M.J. Ammer, J.L. da Silva jr., D. Patel, and S. Roundy, "PicoRadio supports ad hoc ultra-low power wireless networking", *Computer*, pp. 42-48, Jul. 2002.

[5] Y. Yu, R. Govindan, and D. Estrin, "Geographical and Energy Aware Routing: A Recursive Data Dissemination Protocol for Wireless Sensor Networks," Technical Report ucla/csd-tr-01-0023, Computer Science Dept., Univ. of California, Los Angeles, May 2001.

[6] J.N. Al-Karaki and A.E. Kamal, "Routing techniques in wireless sensor networks: A survey", *IEEE Wireless Communications*, pp. 6-28, Dec. 2004.

[7] X. Li, "RSS-based location estimation with unknown pathloss model", Jan. 2005, *IEEE Transactions on Wireless Communications,* 2006, accepted for publication.

[8] N. Patwari, A.O. Hero, M. Perkins, N. Correal, and R.J. O'Dea, "Relative location estimation in wireless sensor networks", *IEEE Trans. on Signal Processing,* vol. 51, no. 8, pp. 2137-2148, Aug. 2003.

[9] X. Ji and H. Zha, "Sensor positioning in wireless ad-hoc sensor networks using multidimensional scaling", *IEEE Infocom*, 2004.

[10] Y. Shang, W. Ruml, Y. Zhang, and M. Fromherz, "Localization from connectivity in sensor networks", *IEEE Trans. on Parallel and Distributed Systems*, vol. 15, no. 11, pp. 961-973, Nov. 2004.

[11] J. Hightower and G. Borriello. "Location Systems for Ubiquitous Computing," *IEEE Computer*. Vol 34, No. 8. August 2001.

[12] J. Hightower, C. Vakili, G. Borriello, and R. Want, "Design and Calibration of the SpotON Ad-Hoc Location Sensing System," August 2001.

[13] P. Bahl, V.N. Padmanabhan, "RADAR: An In-Building RF-based User Location and Tracking System," *INFOCOM* (March 2000) pp. 775-784.

[14] S. Capkun, M. Hamdi, and J.P. Hubaux, "GPS-free positioning in mobile ad-hoc networks," *Proceedings of the 34th IEEE Hawaii Int. Conf. on System Sciences (HICSS-34),* 2001.

[15] K. Whitehouse and D. Culler, "Calibration as Parameter Estimation in Sensor Networks," *In First ACM International Workshop on Wireless Sensor Networks and Application,* Atlanta GA, September 2002.

[16] D. Niculescu and B. Nath, *"*Ad Hoc Positioning System (APS) using AoA," in *Proc. IEEE Joint Conf. IEEE Computer Communications Societies (INFOCOM)*, San Francisco, CA, USA, Mar. 2003, pp. 1734–1743.

[17] D. Niculescu and B. Nath, "DV Based Positioning in Ad hoc Networks," *Journal of Telecommunication* Systems, 2003.

[18] R. Nagpal, H. Shrobe, and J. Bachrach, "Organizing a global coordinate system from local information on an ad hoc sensor network," in *2nd Intl. Workshop on Inform. Proc. in Sensor Networks,* April 2003.

[19] R. Want, A. Hopper , V. Falcão , J. Gibbons, "The Active Badge Location System," *ACM Trans. Information Systems,* Jan. 1992, pp. 91-102.

[20] N. B. Priyantha, A. Chakraborty, H. Balakrishnan, *"*The Cricket Location-Support system," *Proc. 6th ACM MOBICOM,* Boston, MA, August 2000.

[21] N. Bulusu, J. Heidemann and D. Estrin, "GPS-less low cost outdoor localization for very small devices," *IEEE Wireless Communications,* Vol 7. No.5, pp. 27-34, Oct 2000.

[22] A. Savvides, C. C. Han, M. B. Srivastava, "Dynamic Fine-Grained Localization in Ad-Hoc Wireless Sensor Networks," *Proceedings of the International Conference on Mobile Computing and Networking (MobiCom) 2001,* Rome, Italy, July 2001.

[23] Y. Shang, W. Ruml, "Improved MDS-Based localization," *Proceedings of the 23rd Conference of the IEEE Communicatons Society,* Hong Kong , 2004.

[24] J. A. Costa, N. Patwari, and A. O. Hero III, "Distributed multidimensional scaling with adaptive weighting for node localization in sensor networks," *IEEE/ACM*

Trans. Sensor Networks, (to appear). [Online]. Available: http://www.eecs.umich.edu/~hero/comm.html

[25] L. Girod and D. Estrin, "Robust Range Estimation using Acoustic and Multimodal Sensing," In *Proceedings of IROS '01*, Maui, Hawaii, October 2001.

[26] C. Savarese, J. Rabay and K. Langendoen, "Robust Positioning Algorithms for Distributed Ad-Hoc Wireless Sensor Networks," *USENIX Technical Annual Conference,* Monterey, CA, June 2002.

[27] A. Savvides, H. Park and M. Srivastava, "The Bits and Flops of the N-Hop Multilateration Primitive for Node Localization Problems," In *First ACM International Workshop on Wireless Sensor Networks and Application,* Atlanta, GA, September 2002.

[28] K. Whitehouse and D. Culler, "Calibration as Parameter Estimation in Sensor Networks," In *First ACM International Workshop on Wireless Sensor Networks and Applications,* Atlanta GA, September 2002.

[29] K. Pahlavan and A. Levesque, *Wireless Information Networks*, John Wiley & Sons, Inc., 1995.

[30] G. Durgin, T.S. Rappaport, and H.Xu, "Measurements and models for radio path loss and penetration loss in and around homes and trees at 5.85 GHz," IEEE *Journal on Sel. Areas in Comm.,* vol. 46, no. 11, pp. 1484-1496, Nov. 1998.

[31] T.S. Rappaport, *Wireless Communications: Principles and Practice*, Prentice-Hall Inc., New Jersey, 1996.

[32] H. Hashemi, "The indoor radio propagation channel," *Proceedings of the IEEE*, vol. 81, no. 7, pp. 943-968, July 1993.

[33] J. Aldrich, "R. A. Fisher and the Making of Maximum Likelihood 1912-1922," *Statistical Science*, Vol. 12, No. 3 (Aug., 1997) , pp. 162-176.

[34] I.J. Myung, "Tutorial on maximum likelihood estimation," *Journal of Mathematical Psychology,* 47, pp. 90–100, 2003.

[35] W. S. Torgeson, "Multidimensional scaling of similarity," *Psychometrika,* vol. 30, pp. 379--393, 1965.

[36] J. B. Kruskal and M. Wish. *Multidimensional Scaling*. Sage Publications, Beverly Hills, CA, 1978.

[37] M. Steyvers, Multidimensional Scaling. In: *Encyclopedia of Cognitive Science.* Nature Publishing Group, London, UK, 2002.

[38] I. Borg and P.Groenen, *Modern Multidimensional Scaling - Theory and Applications,* Springer, 1997

[39] A. J. Coulson, A. G. Williamson, and R. G. Vaughan, "A statistical basis for lognormal shadowing effects in multipath fading channels," *IEEE Trans. on Veh. Tech.,* vol. 46, no. 4, pp. 494–502, April 1998.

[40] Crossbow Technology Inc. *MICA2 datasheet*. Available July 2006 at http://www.xbow.com/Products/Product_pdf_files/Wireless_pdf/MICA2_Datasheet.pdf

[41] *SmartRF CC1000 Datasheet* (rev. 2.2). Chipcon AS, April 2004. Available April 2004 at www.chipcon.com/files/CC1000 Data Sheet 2 2.pdf.

[42] Crossbow Technology Inc. *MIB510 Datasheet,* Available July 2006 at http://www.xbow.com/Products/Product_pdf_files/Wireless_pdf/MIB510CA_Datasheet.pdf

[43] D. Gay, P. Levis, R.V. Behren, M. Welsh, E. Brewer, and D. Culler, "The nesC Language: A Holistic Approach to Network Embedded Systems," In *Proceedings of the ACM SIGPLAN 2003 Conference on Programming Language Design and Implementation (PLDI)*.

[44] P. Levis, TinyOS Programming.

[45] TinyOS programming tutorial, Available at http://www.tinyos.net/tinyos-1.x/doc/tutorial/ , July 2006.

[46] Crossbow Technology Inc. *MPR-MIB manual,* Available July 2006 at http://www.xbow.com/Support/Support_pdf_files/MPR-MIB_Series_User_Manual_7430-0021-05_A.pdf

[47] A. Koneru, X. Li and M.Varanasi, "Comparative study of RSS-based collaborative localization methods in sensor networks," *The IEEE Region 5 Annual Conference,* April 2006.

[48] Matlab, Available July 2006 at http://www.mathworks.com/products/matlab/